Sensor Technology and Applications to a Real-Time Monitoring System

by

David C. Greene

B.S. Civil and Environmental Engineering
University of California, Berkeley, 2000

Submitted to the Department of Civil and Environmental Engineering in partial fulfillment of the requirements for the Degree of

MASTER OF ENGINEERING IN
CIVIL AND ENVIRONMENTAL ENGINEERING

AT THE

MASSACHUSETTS INSTITUTE OF TECHNOLOGY

JUNE 2001

Author...

David Greene
Department of Civil and Environmental Engineering
May 21, 2001

Certified...

Kevin Amaratunga
Assistant Professor of Civil and Environmental Engineering
Thesis Supervisor

Accepted by...

Oral Buyukozturk
Chairman, Departmental Committee in Graduate Studies

Sensor Technology and Applications to a Real-Time Monitoring System

by

David C. Greene

Submitted to the Department of Civil and Environmental Engineering
On May 21, 2001 in Partial Fulfillment of the
Requirements for the Degree of Master of Engineering in
Civil and Environmental Engineering

Abstract

Large-scale structures such as bridges, dams and buildings have caused countless fatalities in the past decades because engineers were not able to detect the early signs of failure. It is believed that with the implementation of a distributed sensor network, many of these unfortunate events could have been avoided. The ultimate goal in applying distributed sensors is for structures to combine mechanical systems and computer processing to allow them to adapt themselves in extreme conditions without human assistance.

The Flagpole project is attempting to build such a monitoring system by instrumenting a model of a flagpole in a laboratory environment. The selected sensors, accelerometers, strain gauges and thermocouples, provide a complete description of the model's behavior to the physical environment. These sensors stream data into a data acquisition system, which buffers the data and directs it to a database for storage. Visualization software allows for Internet users to view the data in real-time and analyze the model's reaction to current external forces.

For this system to become more automated, new sensor technology must be explored. Recent advances in the field of MEMS technology and wireless communication should be examined to build a system that incorporates decision-making at the sensor level and is expandable to larger scale systems.

Thesis Supervisor: Kevin Amaratunga

Title: Assistant Professor of Civil and Environmental Engineering

Acknowledgements

I would like to first dedicate this thesis to my great-grandfather Albert E. Greene who provided the inspiration for me to come to MIT. His legend will continue to live on in the family.

To all my professors and classmates at the University of California who challenged me and forced me to take my studies to another level.

To my parents, Dan and Suzanne, my brother Jonathan, and sister Christina, thank you for your love and support.

To Prof. Kevin Amaratunga and fellow M.S student, Ragunathan Sudarshan, the Flagpole project would never have made it so far without your dedication.

To all the M.Eng students in the Information Technology track, it was a pleasure working with all of you.

Finally, I would like to thank God for blessing me with the opportunity of pursuing my education this far. Thank you for giving me the strength to persevere through all the difficult times.

Table of Contents

List of Figures

List of Tables

1 Introduction

The purpose of this thesis is to examine the theory and application of some common sensors and how they can be applied to a structural monitoring project. The project to be discussed is a Master's research initiative in the department of Civil and Environmental Engineering at the Massachusetts Institute of Technology (MIT) in Cambridge, Massachusetts. It was given the title Flagpole in tribute of the structure to be monitored, a 100 foot flagpole located in a courtyard outside the Civil and Environmental Engineering building on the MIT campus. The project was created through the funding of Microsoft's I-campus program in June 2000 and presently consists of nine Master's students and a faculty advisor, Prof. Kevin Amaratunga. In looking beyond the monitoring of a flagpole, the Civil and Environmental Engineering Department would like to use this experience as a foundation for future monitoring and decision support system studies at MIT.

This thesis will mainly focus on the sensors that are currently being used on the Flagpole project - thermocouples, accelerometers and strain gauges. It will go into the different components of each sensor and describe their governing physical principles. Keeping in mind future expansions to the research, recent advancements in the area of sensor technology and wireless communication are also covered within the context of monitoring.

1.1 Motivation

One of the biggest oppositions that engineers face in design are the unpredictable forces of nature. On August 17, 1999, Turkey became a victim to a devastating earthquake that that measured 7.4 on the Richter scale. According to a briefing by EQE International, the tremors lasted 45 seconds and in the end there were an estimated 40,000 deaths, and 20,000 buildings with severe damage. The industrial regions of Turkey were heavily damaged, including the Tüpras Refinery in Korfez, which accounts for 1/3 of Turkey's oil. This refinery alone is believed to have totaled $1 billion in damage. According to experts at EQE, almost all damage caused by the earthquake was avoidable (Izmit, Turkey Earthquake Briefing, 1999).

Catastrophic events, such as the Turkey earthquake do not occur everyday, so the amount of information engineers have of these events is limited. The time and location of the next one is unknown, making it hard for engineers to examine the behavior of a structure through the time span of the event. If full time-history information were available at critical points in every structure, the mode and source of failure could be pinpointed and used as lessons in subsequent designs. This is where inexpensive and durable monitoring devices could make a deep impact in the health and longevity of not only structures, but of people as well.

Sensors are a central piece of any monitoring system. They collect information in various forms for engineers and scientists to interpret and make conscious decisions. As technology advances, sensors are becoming cheaper and more compact, facilitating their widespread use in large-scale projects. The role of an engineer monitoring each sensor output becomes unfeasible in a system of hundreds and thousands of sensors. The solution is for sensors to incorporate decision-making and reactive abilities. Such is a major motivation behind the MEMS (Micro-Electro-Mechanical-Systems) and other "smart sensors". NASA has provided a more complete definition to the term 'smart' sensor:

> The sensor itself has a data processing function and automatic calibration/automatic compensation function, in which the sensor itself detects and eliminates abnormal values or exceptional values. It incorporates an algorithm, which is capable of being altered, and has a certain degree of memory function. Further desirable characteristics are that the sensor is coupled to other sensors, adapts to changes in environmental conditions, and has a discrimination function (Ohba, 1992).

Like the human body's capacity to interpret information, sensors are becoming smarter in their ability to incorporate decision-making into their process. As sensors become more human like, they actually reduce the need for human assistance, often leading to a decline in measurement error (Polak, 1999).

2 Flagpole Monitoring Project

2.1 Project Overview

This thesis will involve some specific aspects of the Flagpole project being administered in the Civil Engineering Department at Massachusetts Institute of Technology (MIT). The Flagpole project is attempting to set up a real-time monitoring system of a real-world structure. We have chosen to monitor the dynamic effects of the flagpole located on the west end of Killian Court on the MIT campus. The exact origin, manufacturer and physical properties of the flagpole are unknown; several searches in the school's archives and libraries have returned nothing. Measuring 102 ft. in height with a base diameter of 16 inches, the flagpole stands high above the surrounding buildings.

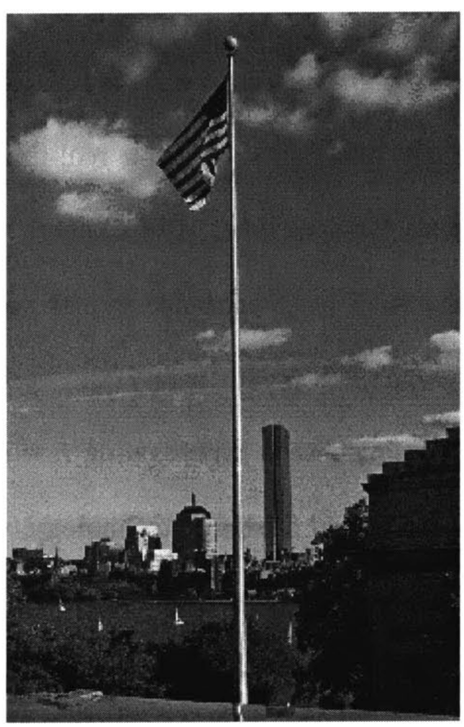

Figure 2.1 – View of flagpole

The faculty advisor for the project is Prof. Kevin Amaratunga with some assistance from Prof. Franz Joseph -Ulm and Prof. Jerome Connor. The three submitted a proposal in March of 2000 to Microsoft for funding of the Flagpole project. Microsoft has made several million dollars available for universities to further improve education through the use of new technologies. The Civil Engineering department saw this as a great opportunity to pursue some new research and attempt to improve its educational system in the same time. Several projects were considered as proposals, including the monitoring of wells and the school's perimeter shuttle bus, before finalizing the proposal with the flagpole. By the summer of 2000, Microsoft decided to fund Flagpole along with seven other projects on the MIT campus. The total financial commitment by Microsoft to MIT totals $25 million over five years.

The Civil Engineering Department would like to expand the concept of setting up a monitoring system to the possibility of using real-time data to build an intelligent decision support system on the structure. The ultimate vision is to have a smart city where all structures could react to catastrophic events such as earthquakes and natural corrosion in hopes of improving public safety and reconstruction costs. The Civil Engineering Department has also been investigating research possibilities in the area of MEMS (Micro-Electro Mechanical Systems) technology, which could be integrated into the flagpole in a couple of years. Along the way we hope to be able to use the information obtained from several sensors installed on the flagpole as teaching tools for basic and complex engineering concepts in mechanics and information technology.

The overall timeline for the Flagpole project is an estimated three years. At the time of this publication, the project has completed ten months of work. The implementation of sensors on the actual flagpole is expected to occur in the next year's phase of the project. To this date, the team has built a simplified structural model to test the sensors and the data acquisition system. Section 2.3 will cover the model in greater detail. Installed on the prototype are three sensors: one accelerometer, two strain gauges and one thermocouple. Further descriptions of these sensors, their applications and alternatives are described in chapter 3. The prototype is also serving as the basis for the educational outreach of the project. Because of its simplicity, it provides an ideal system to teach and demonstrate engineering concepts. Sample programs are displayed further in this chapter.

2.2 System Diagram

The flow of information in the project's monitoring system can be visualized as a cycle divided into three major sections. The first section consists of the structural and hardware components of the project. These include the observed structure, the sensors and a data acquisition system. The second section includes the software solutions to process and store the data obtained from the data acquisition instrument. Finally, the third section is made up of the data visualization and educational tools available on the Internet. While our current system begins with the structure and ends with the Internet user, it is our future goal to give the user, or the sensors, the power to control the structure in response to abnormal conditions, thus closing the system loop.

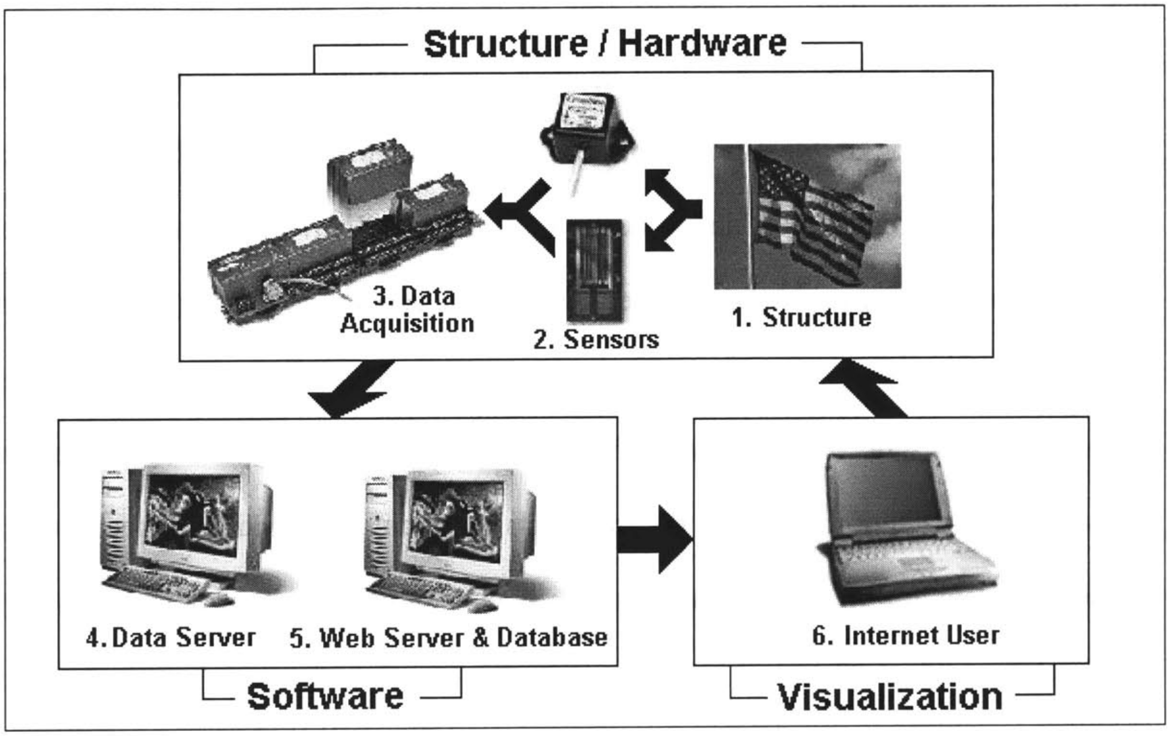

Figure 2.2 - System diagram

Step 1

The system cycle begins with a real-world structure that experiences some sort of measurable change. In the case of a flagpole, the pole and the flag are subjected to wind and drag loads. Detectable deformations in the form of bending and torsion are caused in reaction to these forces. The monitored properties can either come from the structure itself or from the surrounding environment. For example, the model currently monitors both deformation and strain of the shaft as well as the surrounding ambient temperature. The structure is not limited to free standing, building-like structures. As previously mentioned, other proposals for a monitoring system included the monitoring of cars, people and water wells.

In the planning stages of the Flagpole project, the team realized that several barriers prevented the immediate installation of sensors on the flagpole:

1. The team had little experience with the application of sensors.
2. Sensors are expensive and any mistakes in installation would be costly.
3. Because of the height barrier of the tip of the flagpole, there may only be one chance to install the accelerometers.
4. Approval by MIT's physical plant department to alter the aesthetics of the flagpole shell has not been accepted to date.

Because of these issues, we have decided to build a scale model of the flagpole. The model thus has been a basis for the completion of the monitoring cycle which is currently being described. It has also given the team an opportunity to troubleshoot many issues involving sensor installation and sensor selection.

The model is a single degree of freedom upright beam of rectangular cross section. The fixed end of the beam is anchored by four bolts onto an aluminum base. The beam is made of T60-T61 aluminum, which has a density of 2.699 g/cm^3. With a significant width-to-thickness ratio, we can further simplify its movement to be restricted to one degree of freedom. At the tip of the model is located an accelerometer. Chapter 3 will go into detail into the function of the accelerometer. Figure 1.2 shows the dimension details of the model.

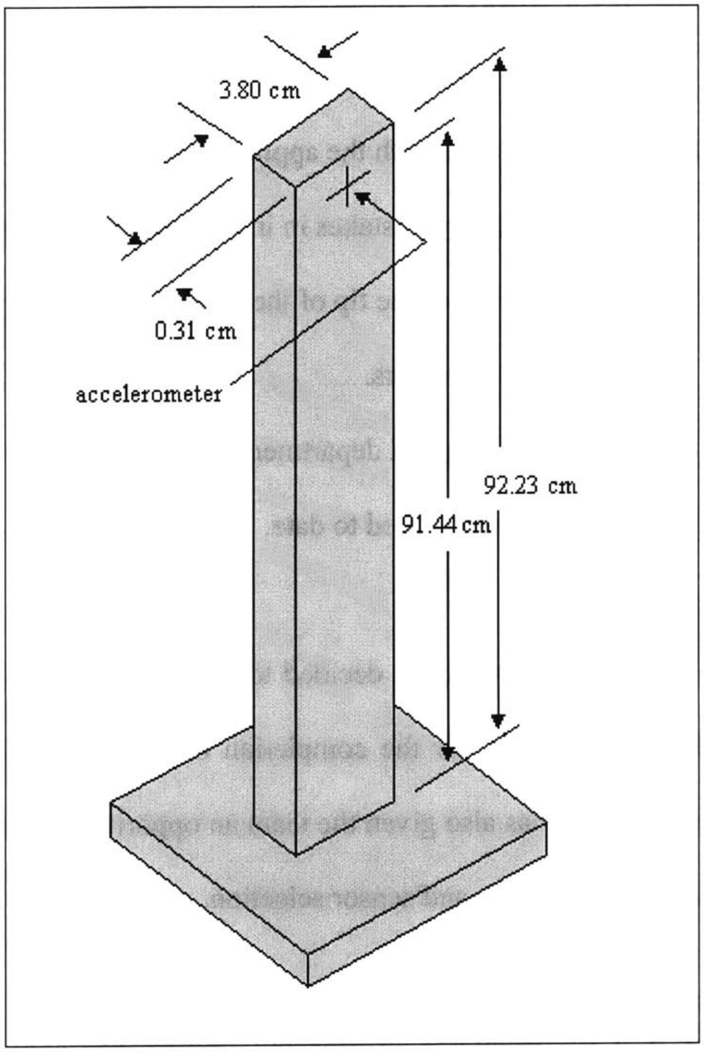

Figure 2.3 – Model dimensions

Step 2

At the location where monitoring is desirable, sensors must be installed to capture the current conditions. Sensors should be selected based on their data range, sensitivity, durability and cost. For the flagpole, as well as the model, the team identified the critical properties to be acceleration, displacement, wind loads, strain, stress, and temperature.

Accelerations and displacements can both be obtained from an accelerometer. Strains and stresses can be obtained from a strain gauge. The wind load is found through the use of an anemometer and temperature is easily measured by using a thermocouple.

When the project is scaled up from the model to the flagpole, new issues arise in the placement of the sensors. Where the model is restricted to one-dimensional movement due to its width-to-thickness ratio, the flagpole is free to move in two dimensions. For the model, the reference axis is easily set perpendicular to the bending axis of the beam. For, the flagpole, there exists no obvious choice of axis based on bending. It is therefore suggested to use the surrounding landscape, namely the encompassing courtyard as a reference.

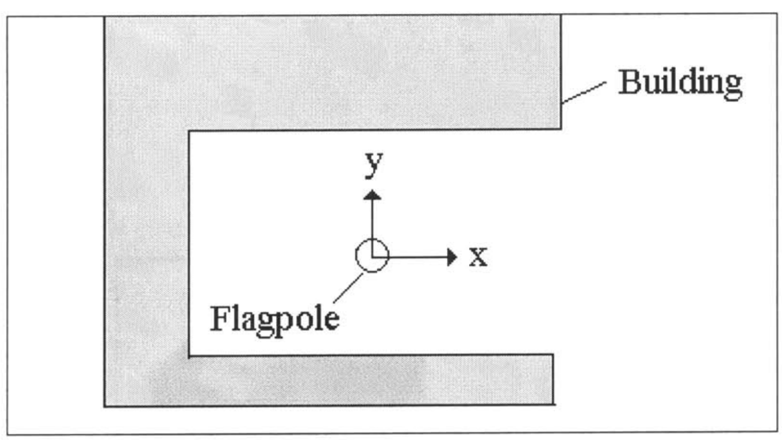

Figure 2.4 – Reference axis for sensors

Step 3

Once sensors are selected that can stream in real-time data, a device is needed to collect the data points. These devices are known as data acquisition systems. The

Flagpole project has utilized a system made by National Instrument called the FieldPoint. In summary, the FieldPoint receives analog data from the various sensors and performs the transformation to a digital signal. The data is then packed and sent off to a PC server. In the case of the Flagpole project, the data is being transmitted at 100 Hz (samples per second).

The FieldPoint system is a modular distributed I/O system. It includes a variety of isolated analog and digital I/O modules, terminal bases, and network interfaces for easy connection to industrial networks, and high-level software tools. One of the main advantages of this system can be found in its architecture flexibility. I/O modules, sensor modules and terminal bases can be mixed to fit the users specific application. Each of the following components can be joined to form a complete data acquisition solution, as seen in Figure 2.5:

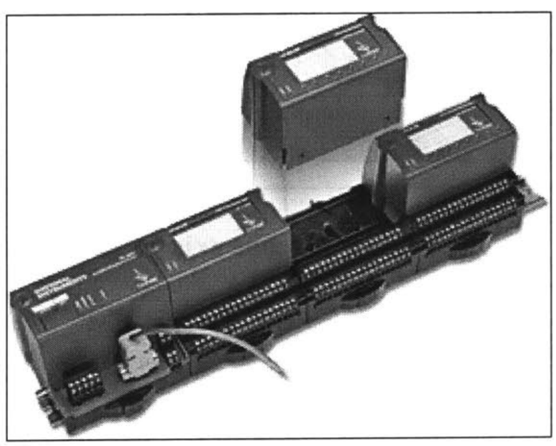

Figure 2.5 – Complete data acquisition system
(FieldPoint from National Instruments, 2001)

I/O Module

I/O modules provide isolated analog and discrete inputs and outputs for a wide variety of signal and sensor types and are hot-swappable and auto-configurable for easy installation and maintenance. The Field Point system includes several types of I/O modules. Discrete modules come in 8- and 16-channel I/O modes and a 4-channel relay mode. Analog I/O modules are also manufactured in 8- and 16-channel I/O modes. The model being used in the Flagpole project is the FP-TB-10 module shown in Figure 2.6. Up to six dual channel I/O modules can be installed on this base.

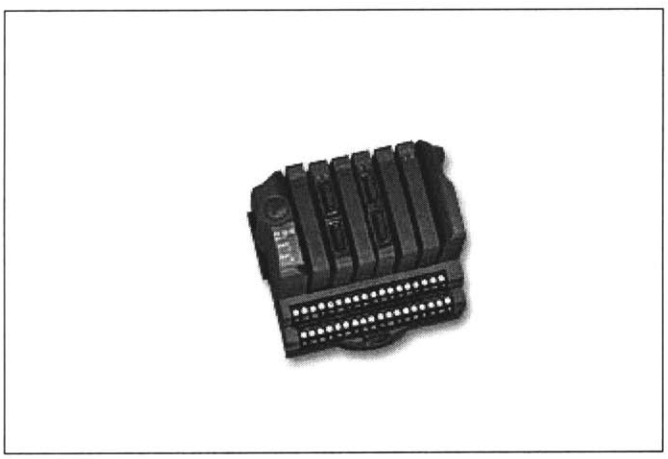

Figure 2.6 FP-TB-10 I/O Module
(FieldPoint from National Instruments, 2001)

Thermocouple Module

A thermocouple module is needed when a thermocouple sensor is used in the system. The model used in Flagpole is the FP-TC-120 module (Figure 2.7). It can handle up to 8 input channels of thermocouples or millivolt signals. Each channel can be configured to handle a different thermocouple type (J, K, T, N, R, S, E, and B) or millivolt range. Other features include self-calibration and rejection of 50/60 Hz Noise. A thermocouple module should be combined with a proper terminal base.

Figure 2.7 FP-TC-120 Thermocouple Module
(FieldPoint from National Instruments, 2001)

Terminal Bases

Terminal bases make up an essential component of the FieldPoint I/O system. They provide connection terminals in the form of screw and spring connections for field wiring, as well as module power and communications. The FP-TB-2 module (Figure 2.8) was selected for the Flagpole system. This particular model has 36 spring terminals for wiring connections.

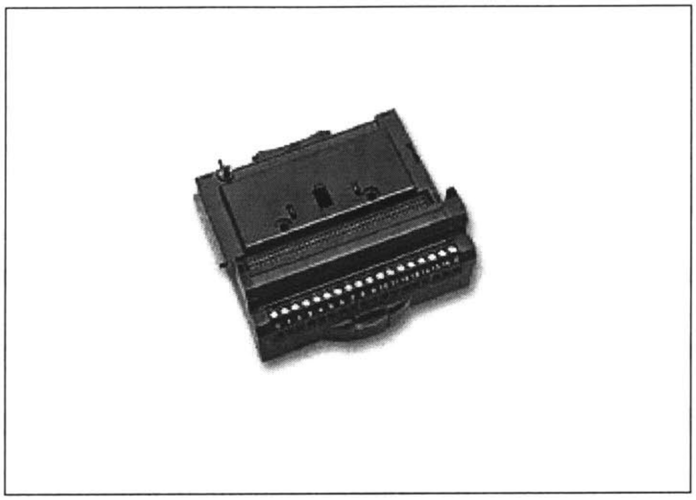

Figure 2.8 FP-TB-2 Universal Terminal Base
(FieldPoint from National Instruments, 2001)

Network Modules

Network modules supply I/O modules with connectivity to open networks. Communication from the network to the local I/O modules is done via the high-speed local bus formed by linked terminal bases. The module also manages communications between the host PC and the I/O modules. The FP-1600 model shown in Figure 2.9 uses an Ethernet TCP/IP interface and provides up to do 100Mb/s data transfer rate.

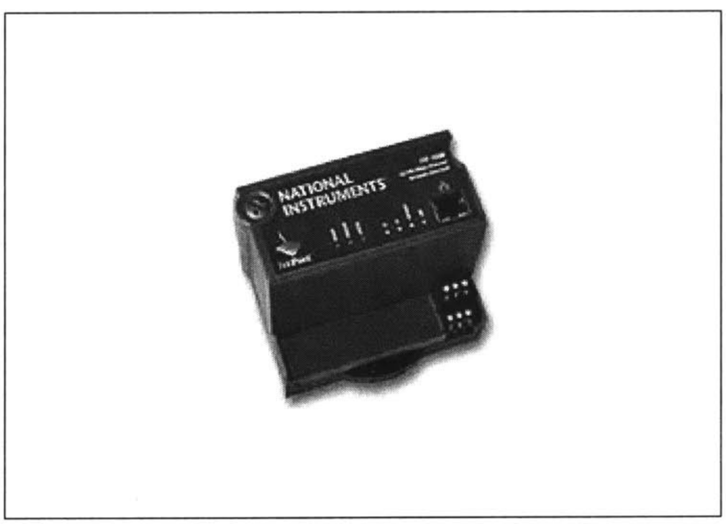

Figure 2.9 FP-1600 Network Module
(FieldPoint from National Instruments, 2001)

Step 4

The next step in the cycle is streaming the information to a data server. The transmission from the data acquisition system to the data server is currently being done through an Ethernet connection. Attempts at wireless transmittals for high sampling rates were unsuccessful because of the limited hardware buffer for accumulating data prior to transmission as network packets. As wireless technology improves over the next couple of years, the wireless route should be re-evaluated.

The data server provides two main functions. First, it utilizes a software package from National Instruments, Lab Windows CVI, that translates the voltage readings into accelerations, strain and temperature values. As will be discussed in Chapter 3, sensors typically output their measurements in voltage values, which need to be converted into significant units. Second, it stores the code to graphical interfaces that allow Internet users to view real-time data. These programs have been written in the Java language and are commonly known as applets.

Once data is transmitted into the data server, it gets allocated to a data socket. Data sockets are temporary storage locations that package the data transmission and make it available to external computers. The data socket implementation can handle up to 16 channels and 16 values per channel, thus they can be viewed as 16x16 arrays. Once the array becomes full, the incoming data points overwrite the old ones.

Step 5

While data is constantly being streamed through on the data socket, a copy of that data is sent to a second computer which functions as the database and web server for the project. The database compresses the data every hour into jar files. Before compression, summaries including averages, high and lows are taken of the set. As a web server, the computer also is home to the project's website, found at http://flagpole.mit.edu. The purpose of the website is to provide information about the Flagpole project, project sponsors, and access to the graphical user interfaces that demonstrate the real-time data in various forms.

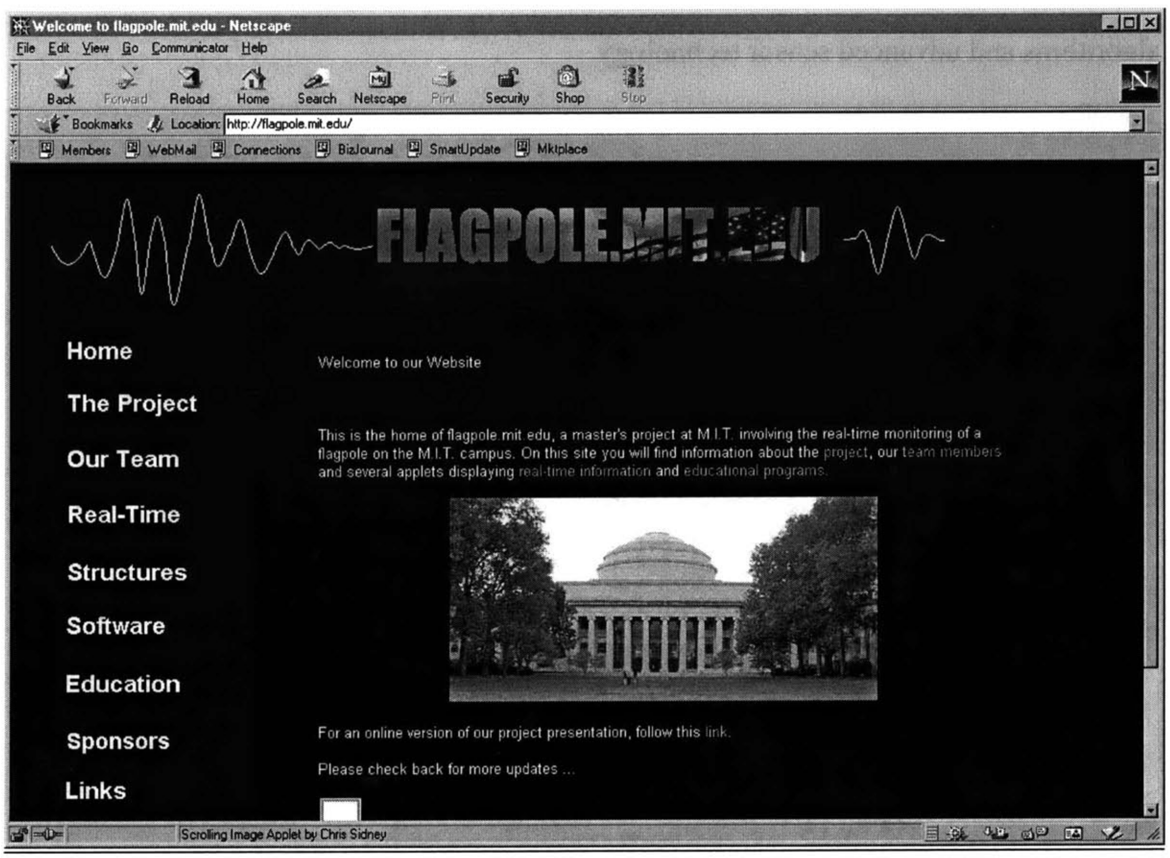

Figure 2.10 – Flagpole.mit.edu (Flagpole Project, 2001)

Step 6

The final step in the monitoring cycle involves the visualization tools that an Internet user will have to choose from. Accessible across the world from any web-ready computer, the collection of applets gives the user an option to view data from any of the sensors. Data is not only viewed in its raw form, but also in a more graphical, user-friendly manner, such as the thermometer shown below in Figure 2.11. Another example is in Figure 2.12, where an applet was created to display a scale model of the flagpole and its dynamic behavior in real-time. The user also plays the role of the decision maker in this cycle. In the case that he or she thinks a current condition is deemed unsafe or critical, then proper action for prevention is taken. It is the future goal of the Flagpole project to have the system gain control of this decision making process by means of smart algorithms and advanced sensor technology.

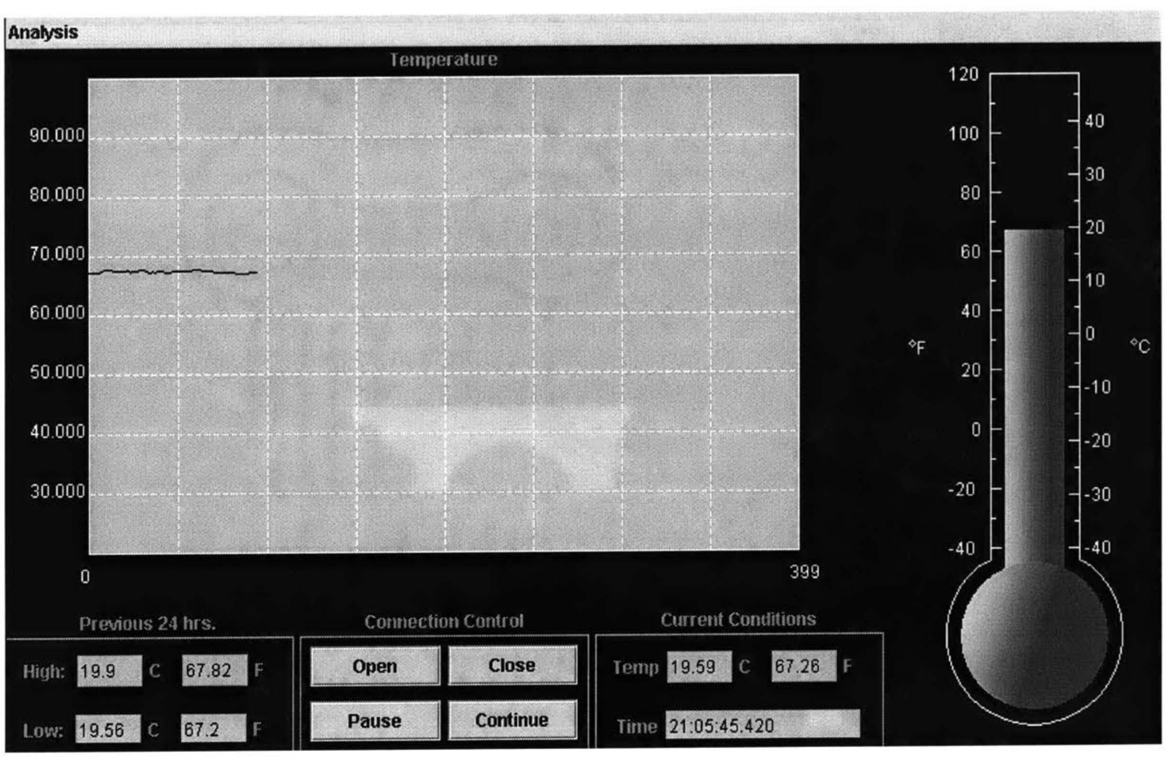

Figure 2.11 – Temperature applet (Flagpole Project, 2001)

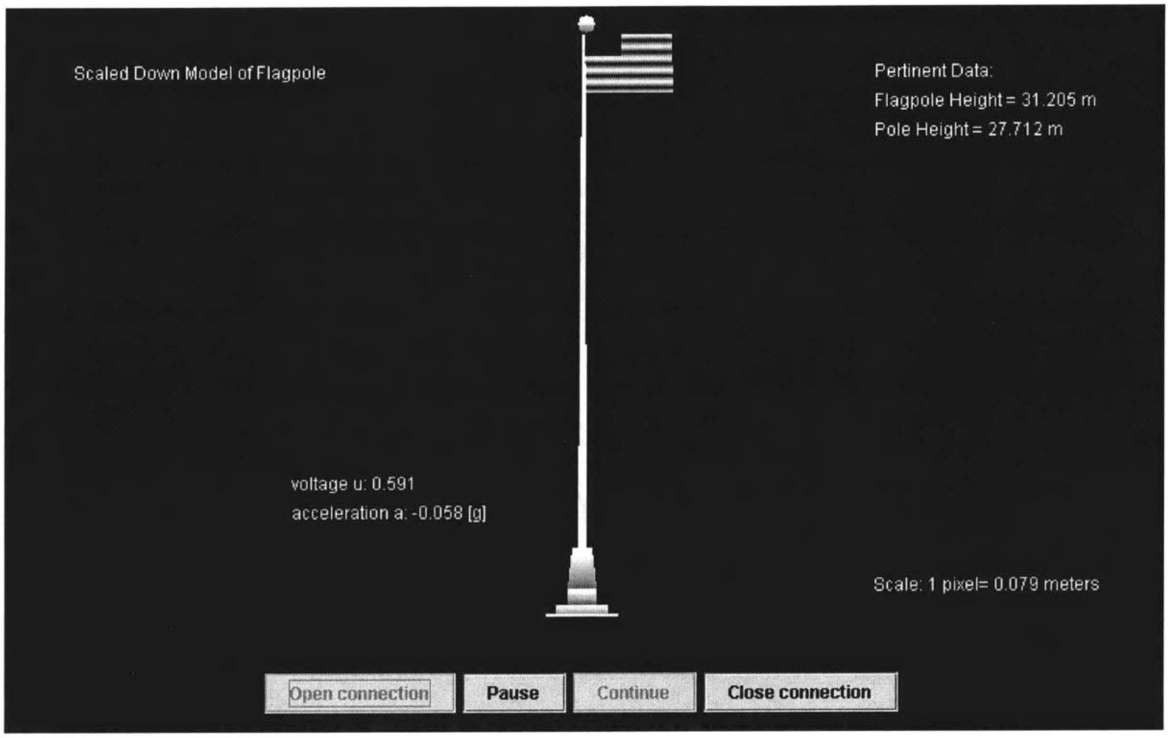

Figure 2.12 – Real-time Applet - Flagpole Simulator (Flagpole Project, 2001)

2.3 Educational Benefits

Though no data has been obtained from the flagpole as of this date, it is clear that when this occurs, the signals will be complex and difficult to decipher. As opposed to the prototype, where we know the signal comes from bending, the flagpole signal will come from a combination of bending, torsion and thermal expansion/contraction. Since we don't know how successful we will be at decomposing the signal into each source, the prototype provides a better structure to aid in the educational aspect of this project. Recall that the funding for the Flagpole project was obtained from Microsoft's Education Fund and therefore providing users with an educational background for the engineering concepts being analyzed is of great importance. For this reason the project contains several online software tools in the form of applets, which describe fundamental engineering concepts in context to the prototype. One example can be seen in the figure below

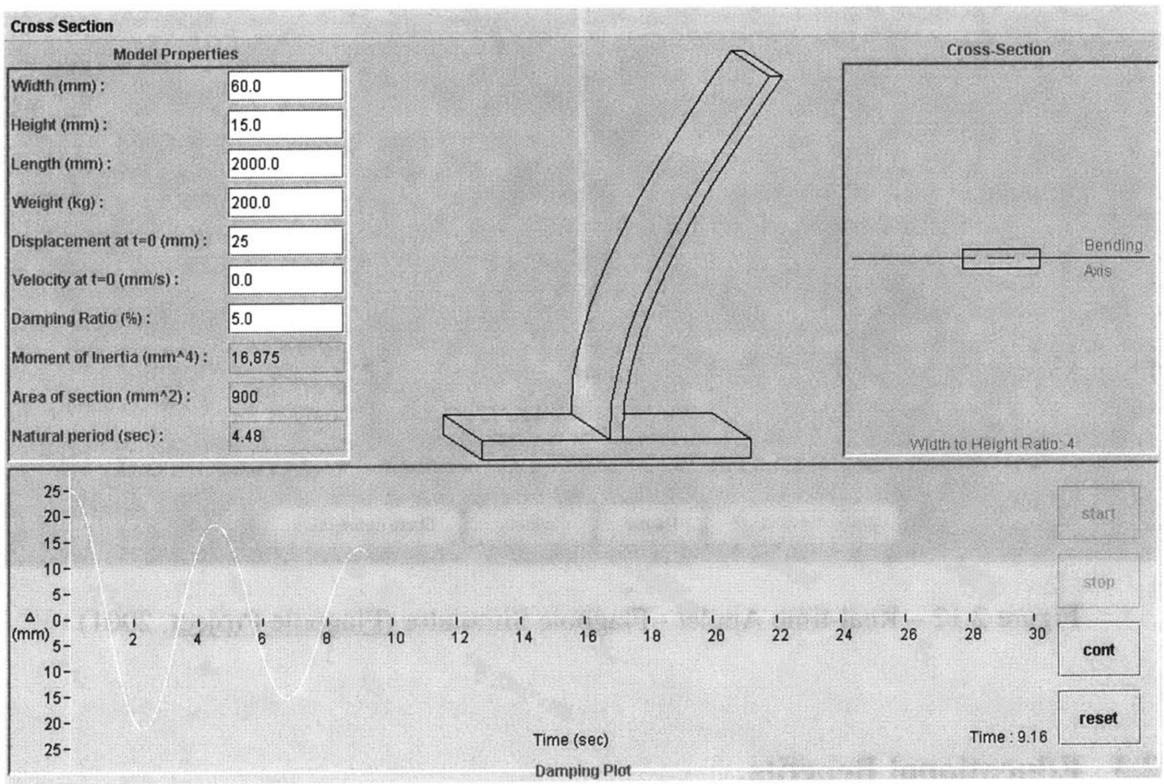

Figure 2.13 – Educational Applet – Damping Behavior (<u>Flagpole Project</u>, 2001)

In this particular program, the user has the option to modify several variables including: width, height, length, weight, initial displacement, initial velocity and damping ratio. Given an initial displacement greater than zero, there is a plotting simulation in the lower portion of the screen that allows the system to be released with initial conditions and oscillate freely. A 3-d model also mimics the theoretical behavior that is dictated by the following equation of motion (Chopra, 1995):

$$x(t) = e^{-\xi w_n t}\left[x_o \cos(w_d t) + \frac{v_o + \xi w_n x_o}{w_d} \sin(w_d t) \right] \qquad \text{Equation (2.1)}$$

where:

x_o – initial displacement at time $t = 0$

v_o – initial velocity at time $t = 0$

w_n – natural frequency of system

w_d – damped vibration frequency

ξ - damping ratio

The user is encouraged to change the parameters and re-run the simulation to gain a greater understanding of the concept of dynamic damping. The Flagpole website currently has several similar educational programs that describe interactively different engineering mechanics principles, including Mohr's Circle, Culmann Method and Tuned Mass-Damper.

3 Sensors

3.1 Introduction

Sensors are devices that have the ability to sense physical properties of the surrounding environment and return outputs that can be significantly interpreted. More simply, sensors input information into a system from the external world (Brignell, 1994). Human bodies have their own sensing mechanisms in the ability to detect sight, hearing, touch, taste and smell, and process the results accordingly. Sensors are categorized in a variety of manners, including their principle of operation, material type and accuracy. Examples of each type are given below:

Principle of Operation	Material Type	Accuracy
Acoustic	Bimetallic	60 dB
Electromechanical	Fiber optic	± 10 g
Hall effect	Silicon	± 1 g
Infrared		

Table 3.1 – Examples of Sensor Classification (Ohba, 1992)

While technology has developed impressive new sensing technology, this Chapter will focus on basic sensors that match the requirements for the Flagpole project. The most relative properties for structural analysis are movement (acceleration and displacement) and forces. The corresponding sensors that produce these measurements are accelerometers and strain gauges. For practice and possibly for data analysis purposes, the project also obtained a thermocouple to measure the ambient temperature near the flagpole. Recent advances in sensing technology and sensor networks will then be discussed in Chapters 4 and 5.

3.1.1 Selection Process

The process of selecting an appropriate sensor should be done carefully. The goal is to get a sensor that produces as a high a signal as possible and with minimum disturbances from other sources. It should be noted that sensors designed to respond to one particular physical variable are often influenced to some degree by other variables. For example, a strain gauge used to detect changes in surface deformation may also respond to changes in temperature. Proper selection of sensors may not completely eliminate the thermal effect, but the deviation can be lowered to within an acceptable range. The communication mode by which the data travels can also significantly alter the quality of measurements and should also be carefully selected (Romberg, 1996).

Ohba (1992) suggests an ordered list of criteria to be used when selecting sensors in the design stage of any monitoring project:

1. Determine the subject of measurement.
2. Set a requirement for the precision and dynamic range that the sensor should handle.
3. Evaluate maintenance needs, cost and compatibility with other sensors in the system.

3.1.2 System Redundancy

While a sensor may label itself to be highly accurate, the means by which it is applied can lead to inaccurate results (Polak, 1999). Errors in measurement may be caused by human misinterpretation, improper connections or faulty components. This unreliability that is present in every system is commonly addressed by distributing sensors and associated hardware components around the structure in order to insure against failure in one localized area. Such an approach is known as hardware redundancy, as sensor outputs are compared to one another for logistical consistency, with small variations between them being ignored. When building hardware redundancy into a system, it is important to remember that identical sensors tend to have similar life expectancies, and therefore any malfunction in a sensor is likely to be followed by the malfunctions in other sensors (Romberg, 1996).

To insure monitoring continuity and reliable results, the Flagpole project plans to incorporate system redundancy in the next scaling phase. The goal will be to place sensors, namely strain gauges and accelerometers, opposite to each other on the pole's cross-section, as shown in Figure 3.1. Due to the symmetry of a circular cross-section, there is no dominant bending axis occurring during motion. The placement of the sensors is therefore left up to the engineer to decide. A suitable choice would be to match the reference axis that was suggested in Figure 2.4. Notice that regardless of bending axis, placing two sensors (accelerometers or strain gauges) 180 degrees apart will yield equal and opposite results.

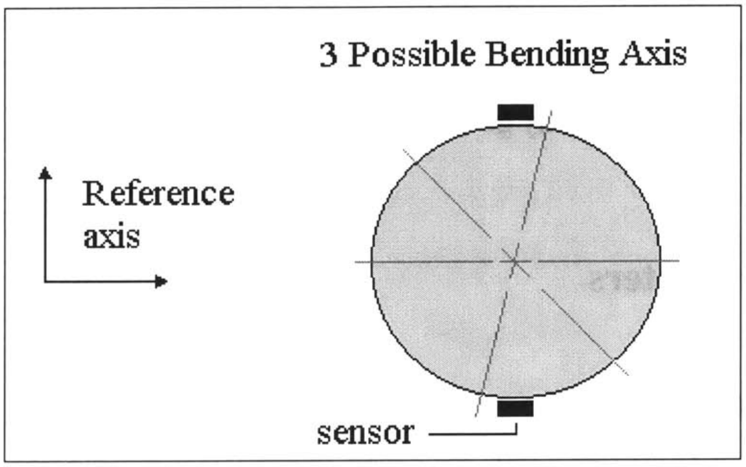

Figure 3.1 – Hardware Redundancy

3.1.3 Sensor Decision Making

As mentioned in chapter 2, the ultimate goal of the Flagpole project is to have a continuous feedback loop. In order to set a standard by which the system follows in making decisions, knowledge of system tendencies (ex. noise patterns) must be obtained. It is suggested by Romberg (1996) to collect sample records over a significant period of time in order to establish a set of "historical standards" where normal behavior can then be defined. Evaluation and identification of system noise is also crucial to the creation of a decision boundary. An ideal boundary should be set high above the background noise level, but not so high that alarming, abnormal conditions remain undetected.

The MIT campus serves as a perfect example for this dilemma. The streets close to the flagpole recently underwent heavy construction, where piles were driven deep into the soil. The machinery caused extensive and noticeable shaking of nearby buildings. Such events would surely alarm any sensitive sensors that may be detecting seismic activities. If the sensor tolerances were raised high enough to neglect the construction noise, small seismic activity may go unattended.

3.2 Accelerometers

3.2.1 Theory

Accelerometers are sensors that convert acceleration from motion or gravity to an electrical signal. In its simplest form, a conventional accelerometer consists of a proof mass, a spring and a position detector. Under steady state conditions, the proof mass experiencing a constant acceleration will move from its rest position to a new position determined by the balance between its mass times the acceleration and the restoring force of the spring. Using a simple mechanical spring, the acceleration will be directly proportional to the distance traversed by the proof mass from its equilibrium position (Brignell, 1994).

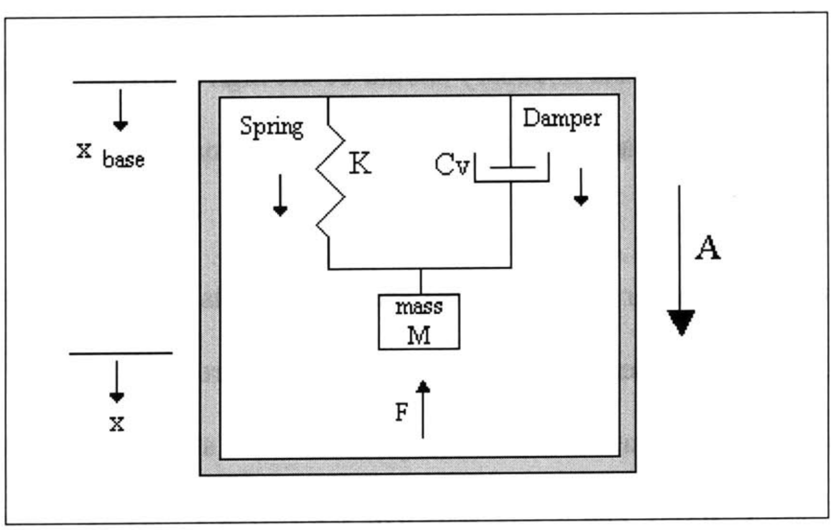

Figure 3.2 - Simple Accelerometer (Brignell, 1994)

The mathematical model of an accelerometer is represented by the following force-acceleration relationship, which can be derived from balancing the forces in Figure 3.2 (Chopra, 1995):

$$F = m\ddot{\eta} + c_v\dot{\eta} + k\eta = ma \qquad \text{Equation (3.01)}$$

where:

$$\eta = x - x_{base} \qquad \text{Equation (3.02)}$$

The undamped natural frequency of the system:

$$w_n = \sqrt{\frac{k}{m}} \qquad \text{Equation (3.03)}$$

The damping ratio:

$$\zeta = \frac{c_v}{2\sqrt{km}} \qquad \text{Equation (3.04)}$$

Acceleration is commonly measured in units of gravity (g), where 1g = 9.80665 m/s^2. Most accelerometers have measuring ranges from 1g to 50g. To gain a better understanding of the units of gravity Table 3.2 shows scenarios where different values of g are reached:

1 g	Acceleration exerted by the Earth's gravity on an object
0 – 2 g	Acceleration experienced when a human moves
5 – 30 g	Acceleration experienced by a driver in a typical car crash
10,000 g	Acceleration of an object shot from a cannon

Table 3.2 – force scenarios in terms of gravitational force (g)

Every calibrated accelerometer should have one definitive resonant (natural) frequency and a flat frequency response where measurements are actually made. Calibration involves determining several characteristics of the accelerometer (Fraden, 1993):

1. Sensitivity, the ratio of the electrical output to the mechanical output, is measured in units of volts per unit acceleration (V/g). In the United States, measurements are done at a reference frequency of 100 Hz.
2. A spectrum of the signal output over the operating frequency range, commonly known as the frequency response.
3. Resonant frequency peak of 3-4 dB higher than the response at the reference frequency should be present for undamped sensors.

Accelerometers, regardless of their driving technology, all rely on the detection of a mass displacement with respect to the outer casing (Fraden, 1993). Several types of accelerometers use this principle in combination with other unique physical principles, as outlined in the following sections

3.2.2 Capacitive Accelerometers

A capacitive accelerometer, like any basic accelerometer, contains a free internal mass and a stationary casing. Attached to the mass and casing are two plates that form a capacitor. The distance between the plates can determine the capacitance of this capacitor (Fraden, 1993):

$$C = \frac{\varepsilon_o A}{d} \qquad \text{Equation (3.05)}$$

To compensate for drifts and interferences, a second capacitor is formed within the casing. Figure 3.3 shows a side view of a capacitive accelerometer. The upper plate and the base, micromachined from silicon, are separated by the distances d_1 and d_2. The silicon springs serve as supports for the mass and determine the acting force by the spring constant of silicon, k.

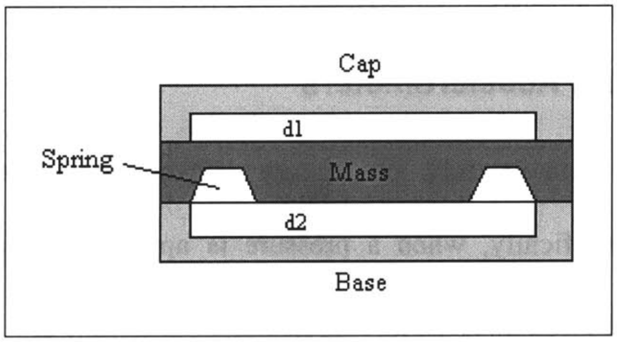

Figure 3.3 – Side-View of Capacitive Accelerometer (Fraden, 1993)

The two capacitors formed are C_{mc}, between the cap and the mass, and C_{mb}, between the mass and the base. Finally, the output voltage is determined (Fraden, 1993):

$$V_{out} = 2E\frac{C_{mc} - C_{mb}}{C_f} \qquad \text{Equation (3.06)}$$

where E is the power supply voltage.

3.2.3 Piezoresistive Accelerometers

Piezoresistive accelerometers obtain accelerations through the use of strain gauges placed on the mass-supporting springs. If the strain on a spring is known, then the displacement and force on the spring are known as well. An advantage of these sensors is their capability to withstand overshock. While some designs can handle up to 10,000g, most piezoresistive accelerometers are suitable for the ±1,000 g range, where 1% accuracy can be expected. Their drawback is found in the tendency to conduct thermal interference by the epoxy-bonded strain gauges. Separate thermal testing is required for each gauge. Common piezoresistive designs have a free mass supported by hinges on the casing. System redundancy is utilized here, as gauges are placed in either side of the mass to simultaneously measure compressive and tensile strains upon movement (Fraden, 1993).

3.2.4 Piezoelectric Accelerometers

Piezoelectric sensors rely on energy conversion between mechanical and electrical form. Specifically, when a pressure is applied to a polarized crystal, the resulting mechanical deformation results in an electrical charge. Like the capacitance accelerometer, two plates are placed on either side of a crystal causing a capacitance, C. The electrical charge, Q_f, results in a voltage also related to this capacitance (Putnam, 1996):

$$V = \frac{Q_f}{C} \qquad \text{Equation (3.07)}$$

The most popular crystals for sensing elements are ceramic piezoelectric materials, such as barium titanate, lead zirconite titanate (PZT) and lead metaniobite (Fraden, 1993). When miniature sensors are required, micromachining technology is utilized to build silicon elements. Chapter 4 will discuss silicon sensing technology in greater detail. While silicon lacks piezoelectric properties, thin films of lead titanate can be placed on the silicon elements. Other advantages of piezoelectric sensors include high linearity, good off-axis noise rejection, and a high temperature tolerance (up to 120°C) (Fraden , 1993).

3.2.5 Accelerometer Application

Accelerometers are used for three main measuring applications: tilt/inclination, inertial forces, or shock/vibration. Tilt accelerometers will not be discussed as they often use liquids as their sensing element.

3.2.5.1 Inertial Applications

Inertial accelerometers are used to measure acceleration, velocity, displacement and force. This is accomplished by integrating the acceleration function to obtain velocity, and once again to obtain a displacement function. Inertial applications include airbag crash sensors, car navigation systems and elevator controls (Accelerometers, 2001).

The Flagpole project is currently using an inertial accelerometer manufactured by Crossbow Technology on its model: It is a high stability LP series with a measuring range of ± 10 g. This particular model (CXL10LP1) comes in both uniaxial and triaxial versions, meaning it can either read acceleration in one dimension, or in three dimensions. The underlying physical principle behind this accelerometer is a capacitance beam with a non-linearity of 0.2 %. Other important specifications include (Accelerometer Overview, 2001):

- Factory calibrated
- Silicon micromachined sensing element
- Sensitivity: 200 mV/G
- Resolution: DC- 100Hz
- Noise: 10 mGrms

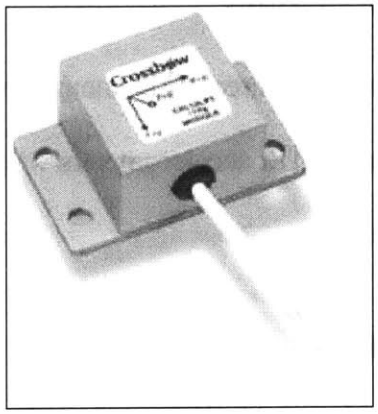

Figure 3.4 – Crossbow accelerometer (model #CXL10LP1)
(Accelerometer Overview, 2001)

3.2.5.2 Vibrational Applications

While the Flagpole project only has the need for inertial sensing, vibrational accelerometers play an important role in the field of structural monitoring. Their most common application is in measuring the "health" or condition of machinery. A simple, steady sinusoidal vibration signal has a specific value of frequency and a specific value of displacement. However, vibrations are commonly made of unsteady signals, containing a complete mixture of frequencies, often varying with time (Polak, 1999). Vibrations can be expressed in three quantitative measures (Ohba, 1992):

1. Wave motion – displacement, speed, acceleration, energy and shape of wave.
2. Time waveform – sine wave motion, random vibrations and impulse vibrations.
3. Instantaneous value, peak value, p-p value, effective value, period and frequency.

Both piezoelectric and piezoresistive accelerometers provide good measuring capacity for vibrational settings. When signals of low-frequency response (less than 5 Hz) are to be measured, piezoresistive sensors are recommended over piezoelectric.

Acceptable levels of vibration depend on the machine's size, and also on the mounting mechanisms and foundations. Vibration measurements may vary significantly depending on the axis of measurement. Despite the precision available in vibration measurements, interpretation of the results is not so straightforward. Making judgments about the health of a particular structure from a single set of data points can be inconclusive, even when comparing to readings of similar machines. This is because there are several factors that contribute to vibration readings: manufacturing tolerances, minor differences in mountings, minor differences in operational conditions, etc. A solution to this problem is performing a spectral analysis of the vibration signal to identify specific troubling frequencies (Polak, 1999). In unsteady signals, identifying trends is more valuable than single sets of measurements.

The lessons learned from monitoring manufacturing equipment with vibrational sensors can be translated into the field of structural monitoring. The National Research Council describes the Life-Cycle Management (LCM) as the monitoring of product design from birth-to-death. It emphasizes the need for new sensor technology which can withstand a long period of usage without calibration or replacement needs. The concept of maintenance-free service does not only apply to the attached sensors, but also to the structure. In the case of fatigue cracks on airplane wings, the Air Force has found their solution in active sensors (National Research Council, 1995). Cracks are normally repaired with a composite boron/epoxy patch. The composite strengthens greatly after application and actually exceeds the strength of the aluminum structure. The problem is when the patch degrades with use and re-exposes the crack. By attaching transducers to the crack, ultrasound waves are constantly generated. When the bond degrades, the ultrasonic pulse spectrum changes as well, alarming engineers that further repair is needed.

3.3 Acceleration Conversions

In the case of many inertial and vibrational applications, displacement and velocity may also be of importance to the system. While accelerations can be directly linked to the external force that the environment is applying on a system, displacements give the engineer a more familiar measure of how the structure is reacting under the applied loads.

3.3.1 Acceleration-Displacement Relationship

The relationship between acceleration and displacement functions are linked through the velocity function. The principles of motion show that the integral of the acceleration function is equal to the velocity function over the same period of time. Mathematically, this relationship can be shown through the following equations:

$$\int a(t)dt = v(t) \tag{3.08}$$

Or in reverse:

$$\frac{dv}{dt} = a(t) \tag{3.09}$$

The integral of a function can also be interpreted as the area under the integrating function. Graphically, this concept is shown in figure 3.5. Note that the area up to time T_i does not equal the velocity V_i, but the difference of V_i and V_o.

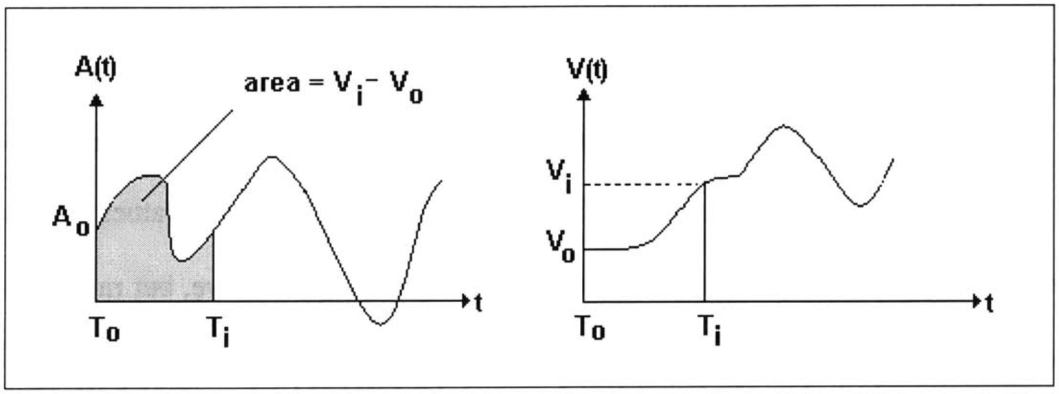

Figure 3.5 –Relationship between acceleration and velocity

The same procedure can be used to determine the displacement function. When the velocity function is now integrated, the resulting function represents the displacements over the same period of time. Again, mathematically this relationship is shown by:

$$\int v(t)dt = u(t) \tag{3.10}$$

$$\frac{du}{dt} = v(t) \tag{3.11}$$

The graphical representation is similar to the acceleration-velocity transformation:

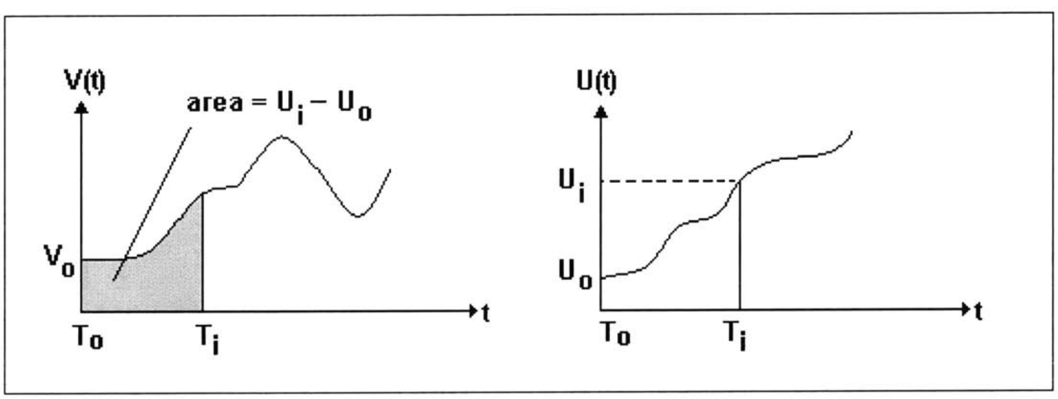

Figure 3.6 Relationship between velocity and displacement

3.3.2 Integration Methods

Recall that the accelerometers used in the Flagpole project are obtaining samples at a rate of 100Hz (samples per second). This translates into missing values in between each sample. The acceleration function will not be a continuous curve, but rather a set of points that resemble a continuous function as in Figure 3.7:

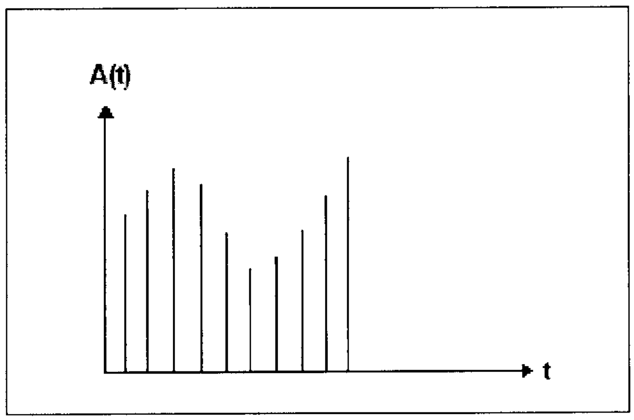

Figure 3.7 – Discrete acceleration function

In order to obtain the area under the function for integration, some assumptions must be made about the values in between samples. There are several integration methods that make certain interpolations to the unknown values. The following sections will describe some of these procedures.

3.3.2.1 Zero-Order Hold

The simplest assumption that can be made is to assume that the signal retains the level dictated by the previous sample. Other terms for this procedure include the Staircase and the Boxcar method. Figure 3.8 shows the zero-order hold being placed on a set of five data points:

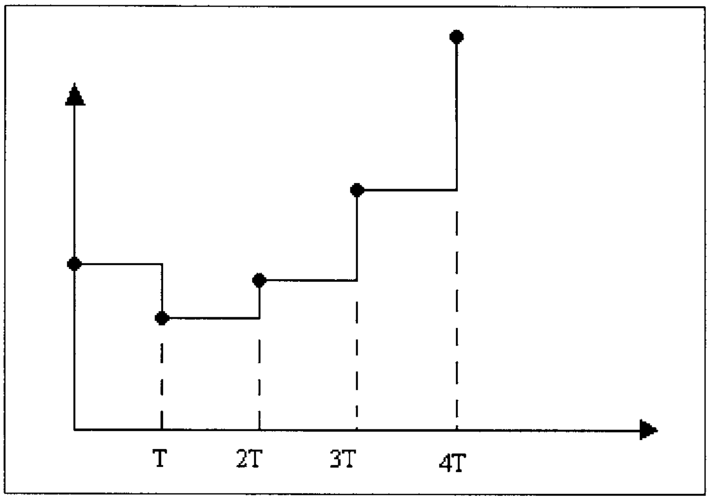

Figure 3.8 – Zero-order hold

Applying the zero-order hold for the integration of an acceleration function will yield:

$$v_i = v_{i-1} + a_{i-1}T \qquad \text{Equation (3.12)}$$

Repeating the step to obtain displacements:

$$d_i = (v_i - a_{i-1}T)T + d_{i-1} \qquad \text{Equation (3.13)}$$

3.3.2.2 Midpoint Rule

This method is very similar to the zero-order hold, except that it assumes the average value between the points as the horizontal interpolation. The main difference between the two methods is Midpoint's dependency on the latter known value, which will be common in most other interpolations made. The same set of points using the midpoint rule is shown in Figure 3.9:

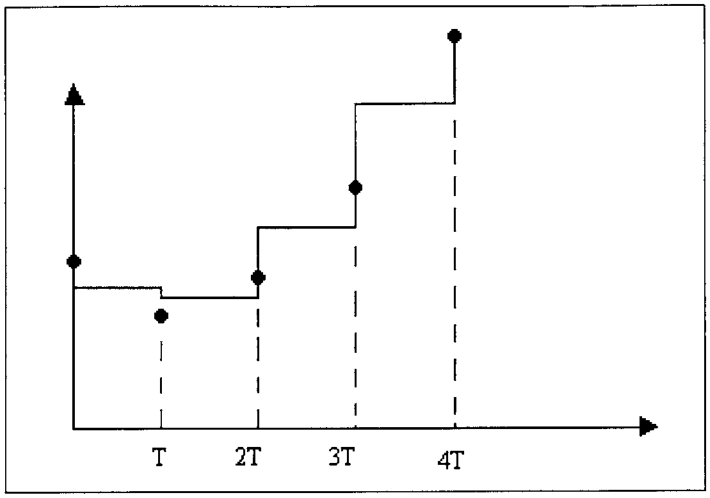

Figure 3.9 – Midpoint Rule

Integrating the acceleration function by means of the midpoint rule yields (Chopra, 1995):

$$v_i = v_{i-1} + \frac{(a_i + a_{i-1})T}{2} \qquad \text{Equation (3.14)}$$

Again,

$$d_i = d_{i-1} + v_{i-1}T + \frac{(a_i + a_{i-1})T^2}{4} \qquad \text{Equation (3.15)}$$

3.3.2.3 Central Difference Method

This method is based on a finite difference approximation of the time derivative of displacement. Instead of beginning with the acceleration function, we begin with the displacements and derive accelerations. Graphically, the central difference method looks as follows:

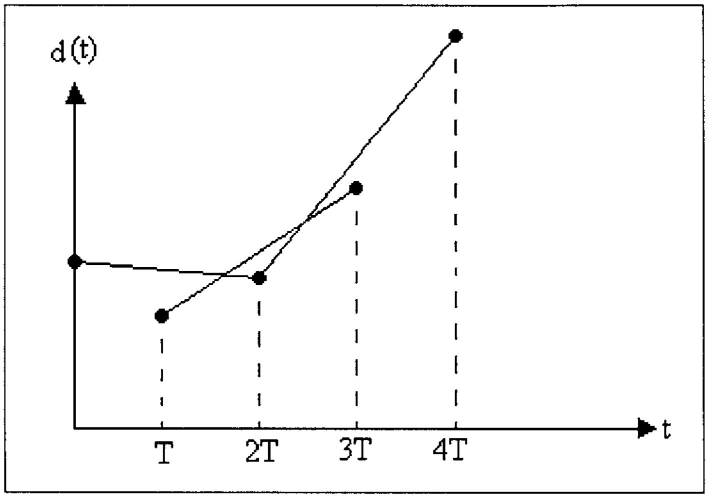

Figure 3.10 – Central Difference Method

Applying this procedure to the velocity function results in (Chopra, 1995)

$$v_i = \frac{d_{i+1} - d_{i-1}}{2T} \qquad \text{Equation (3.16)}$$

and consequently the acceleration function will be represented as:

$$a_i = \frac{d_{i+1} - 2d_i + d_{i-1}}{T^2} \qquad \text{Equation (3.17)}$$

While this procedure is suited for obtaining accelerations given displacement values, Equation 3.17 can be solved for displacements in terms of accelerations by using a time shift:

$$d_i = a_{i-1}T^2 + 2d_{i-1} - d_{i-2} \qquad \text{Equation (3.18)}$$

Central differences have the advantage of bypassing velocity, but they do require some additional assumptions made at the beginning of the iteration. Notice that the iteration can only begin at the third displacement value. This requires knowing the displacements at the first and second time positions. If the structure is at rest when the iteration begins, then assuming a zero value may not affect results significantly. Regardless, it is up to the engineer to decide the precision of his/her calculations.

3.3.2.4 Piecewise Linear Interpolation

Piecewise Linear Interpolation is a method which simply creates a straight line between the known values. This method is also commonly known as the Trapezoidal Rule. Figure 3.9 shows the same set of points using linear interpolation:

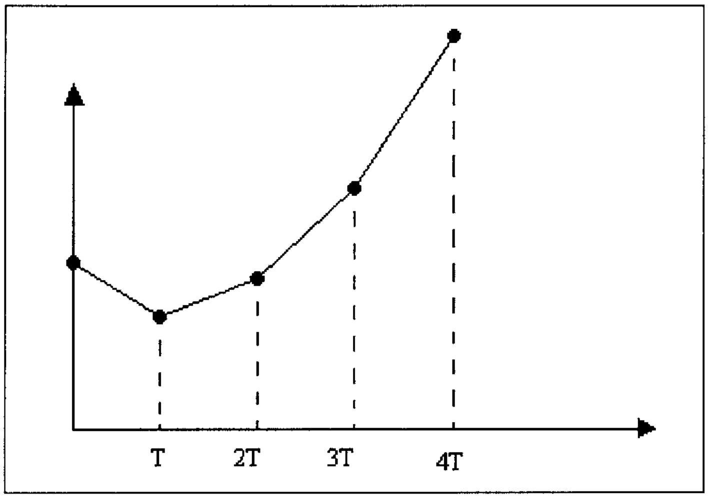

Figure 3.11 – Linear Interpolation

To form an iteration from this method we first solve the velocity function (Chopra, 1996):

$$v_i = v_{i-1} + \frac{(a_i + a_{i-1})T}{2} \qquad \text{Equation (3.19)}$$

likewise,

$$d_i = d_{i-1} + v_{i-1}T + T^2(\frac{1}{6}a_i + \frac{1}{3}a_{i-1}) \qquad \text{Equation (3.20)}$$

3.3.2.5 Sample Code

Once an interpolation technique has been chosen for the double integration, translation into a computer language should be straightforward. For this example, the midpoint rule will be used to demonstrate the sample computer code being utilized in the Flagpole project. Notice that equation 3.15 not only depends on the current acceleration, which the team has streaming from the accelerometer, but also from the previous acceleration, velocity and displacement values. For the first pass through the iteration the parameters must be initialized to some value at t = 0. In the case of the model where human control of the structure is possible, it makes the most sense to set all values to zero. When the project is scaled up the flagpole, it will be a difficult task initializing the parameters to begin the integration. Here's a sample code utilizing a FOR loop to obtain velocity and displacement values:

a(0) = 0;
v(0) = 0;
u(0) = 0;

FOR $(i = 0, i < \max, i = i + 1)$
{

$$v(i) = \left(\frac{a(i) + a(i-1)}{2} \right) \Delta t + v(i-1);$$

$$u(i) = \left(\frac{\left(a(i) + a(i-1)\right)}{4} \Delta t + v(i-1) \right) \Delta t + u(i-1);$$

}

Figure 3.12 – Sample code for midpoint rule

3.4 Strain Gauges

Strain gauges are sensors that measure surface deformation due to bending, torsion and/or thermal expansion and contraction. Knowledge of material properties and dimensions can be combined with strain readings to determine displacements and forces on the structure. Strain, ε, is typically measured in deformation per unit of length of the gauge (Popov, 1990)

$$\varepsilon = \frac{L - L_o}{L_o} \qquad \text{Equation (3.21)}$$

where L_o is the length of the gauge at rest.

3.4.1 Theory

A strain gauge is a resistive elastic sensor whose resistance is a function of the applied strain. The principle of electrical resistance was first discovered in 1856 by Lord Kelvin (Brignell, 1994). He observed that the resistance of various metal wires changed when strained. The resistance of a metallic alloy can be measured as (Brignell, 1994 and Fraden, 1993)

$$R = \frac{\rho l}{A} \qquad \text{Equation (3.22)}$$

where l = length

A = cross-sectional area

ρ = resistivity

Taking the logarithmic differentiation and considering the change in cross-sectional area when a specimen is elongated leads to another relationship:

$$\frac{dR}{R} = \frac{d\rho}{\rho} + (1 + 2\nu)\varepsilon \qquad \text{Equation (3.23)}$$

The sensitivity of a material to an applied strain is defined as the gauge factor, S:

$$S = \frac{dR / R}{\varepsilon} \qquad \text{Equation (3.24)}$$

Combining Equations 3.23 and 3.24 yields

$$S = \frac{d\rho / \rho}{\varepsilon} + (1 + 2\nu) \qquad \text{Equation (3.25)}$$

The gauge factor is made up of two distinct sources. First is the piezoresistive effect - $(d\rho/\rho)/\varepsilon$, and second is the geometric effect $(1+2\nu)$. Table 3.3 lists some common strain gauge materials along with their respective sensitivity factors (Strain Gage - Sensitivity, 2001):

Material	Sensitivity (S)
Platinum	6.1
Platinum–Tungsten	4.0
Constantan / Advance / Copel	2.1
Karma	2.0
Manganin	0.47
Nickel	-12.1

Table 3.3 – Common Sensitivity Factors

The change is resistance of the strain gauge is then detected using a Wheatstone Bridge to obtain an output voltage:

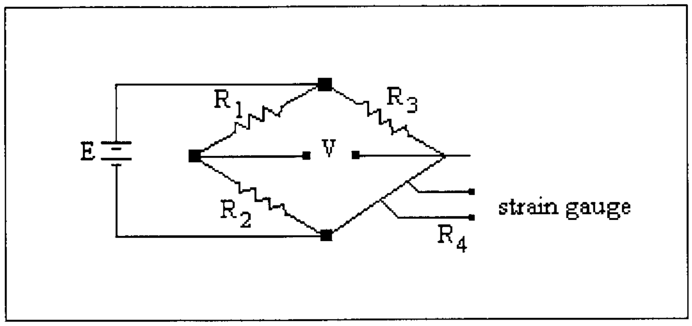

Figure 3.13 – Wheatstone Bridge (Ohba, 1992)

The output voltage, V, is determined by the following equation (Wheatstones Bridges – Introduction, 2001):

$$V \approx \frac{r}{(1+r)^2}\left[\frac{\Delta R_1}{R_1}-\frac{\Delta R_2}{R_2}+\frac{\Delta R_3}{R_3}-\frac{\Delta R_4}{R_4}\right]E \qquad \text{Equation (3.26)}$$

where

$$r=\frac{R_3}{R_4}=\frac{R_2}{R_1} \qquad \text{Equation (3.27)}$$

when the bridge is initially balanced. The coefficient on equation 3.26:

$$\frac{r}{(1+r)^2} \qquad \text{Equation (3.28)}$$

is the known as the circuit efficiency.

3.4.2 Foil Strain Gauge

Figure 3.14 shows a typical foil strain gauge. The grid consists of several parallel wires, resulting in a total gauge length much larger than the active length. Strain gauges are normally available with an active length (gauge length) ranging from 2 to 13 mm (Polak, 1999). The shape of the grid is produced with photochemical technology. The backing is made out of a polyimide film, resulting in a strong, yet flexible resistance. It is applied directly to the surface where strain measurement is desired. The coefficient of thermal expansion of the backing should match that of the wire used (Fraden, 1993). Alignment tabs are often placed on the backing for installation ease.

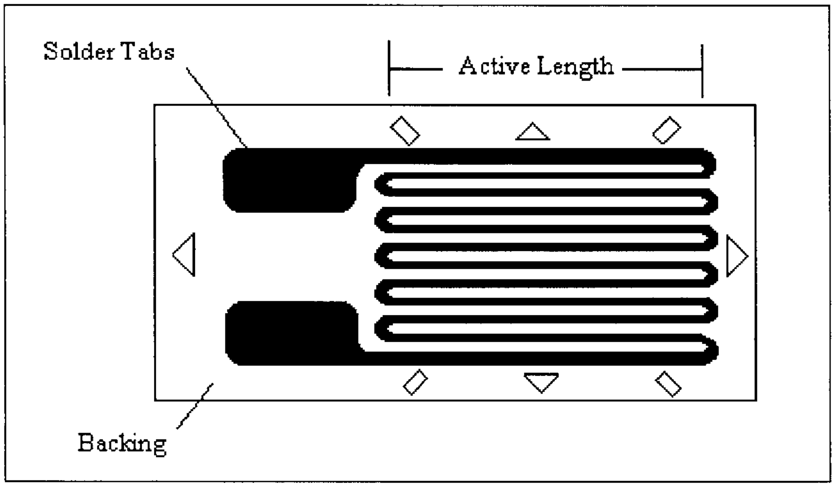

Figure 3.14 – Metal Foil Strain Gauge (Fraden, 1993)

The most common strain gauge wire used is Constantan. Among its benefits is a high electric resistivity, ρ = 0.49 $\mu\Omega\cdot$m, and a low temperature induced strain, in the range of -30 to 193 °C (-20 to 380 °F). Annealed Constantan can also be used in plastic deformations, where strain exceeds 5% (Strain Gage - Sensitivity, 2001).

Isoelastic wires are used when a high signal-noise ratio is necessary and dynamic strains are to be measured. They are, however, highly sensitive to temperature fluctuations, therefore application should be made in a controlled temperature environment, such as an air-conditioned laboratory (Strain Gage – Sensitivity, 2001). For this reason, Isoelastic may not be suitable for the Flagpole project, as the weather in Cambridge, Massachusetts varies substantially from winter to summer.

Karma wires are more similar to Constantan. They possess a self-temperature compensation property in the range of -73 to 260 °C (-100 to 500 °F). Karma wires also have a higher cyclic strain resistance than Constantan (Strain Gage – Sensitivity, 2001).

3.4.3 Types of Strain Gauges

Strain gauges are available in several patterns to suit the needs of each job. All patterns use the basic uniaxial gauge in Figure 3.14 to form combinations, either directly superimposed or with gauges side-by-side. Strain gauge combinations, regardless of form are known as rosettes. The most common patterns include:

- 0°-90° T Rosette – two side-by-side uniaxial gauges with one of its wires in a perpendicular direction to the other, as shown in Figure 3.14.

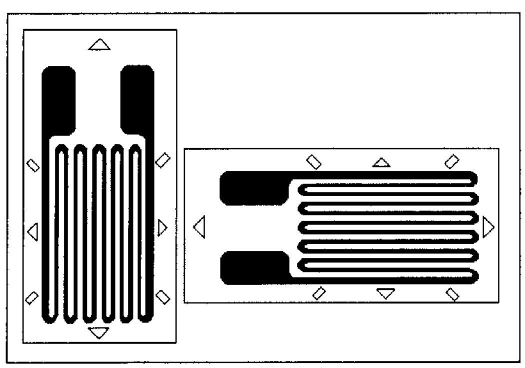

Figure 3.15 - 0°-90° T Rosette

- 0°-45°-90° Rectangular Rosette – like the previous example, except a third gauge is directed at 45 degrees from the other two.

- 0°-60°-120° Delta Rosette – three uniaxial gauges with their gauges directed 120 degrees from each other.

These three patterns are available in either a stacked form, where the gauges are actually superimposed on each other, or in planar form, where the gauges are place either side-by-side or in a circular fashion. Planar layouts have fewer problems with heat dissipation and produce more accurate results, as the gauge wire has no interference with the measuring surface. Stacked layouts are necessary when space is a limitation or a large strain gradient is expected (Strain Gage - Pattern, 2001).

3.4.4 Strain Gauge Calibration

The process of calibrating sensors includes verifying the actual outputs to predicted theoretical solutions. In the case of the model being used by the Flagpole Project (Figure 2.3), the relationship between the tip displacement and the strain value at any point can be calculated through a series of mechanical principles (Popov, 1990):

Stiffness (k) $$k = \frac{3EI}{L^3}$$ Equation (3.29)

Moment of Inertia $$I = \frac{bh^3}{12}$$ Equation (3.30)

Bending Stress (σ) $$\sigma = \frac{Mc}{I} = \frac{(Fd)(h/2)}{I}$$ Equation (3.31)

Force-Stiffness Relationship $$F = k\Delta$$ Equation (3.32)

Stress-Strain Relationship $$\sigma = E\varepsilon$$ Equation (3.33) where:

k- stiffness of beam

E – Modulus of Elasticity

I – Moment of Inertia

b – base, or width of cross-section

h – height, or thickness of cross-section

L – length of beam

F – force applied at tip

σ - stress at distance d from tip

Δ - tip displacement

Combining equations 3.29, 3.30, 3.31, 3.32 and 3.33 yields the final relationship between the tip displacement and the strain:

$$\varepsilon = \frac{3hd\Delta}{2L^3} \qquad \text{Equation (3.34)}$$

Upon giving an initial displacement at the tip of the model, one should be able to predict the strain value anywhere on the shafts outer face.

3.5 Thermocouples

3.5.1 Theory

Thermocouples are the most widely used temperature sensor in test and development work. T.J. Seebeck first discovered the concept behind thermocouples in 1831 (How Thermocouples Work, 2001). He found that current flows when any two wires made of different materials are joined in a closed circuit and heated at one junction. The current will continue flowing as long as the ends are kept at different temperatures. The magnitude and direction of the current are a function of the temperature difference between the junctions and of the thermal properties of the metals used in the circuit (also known as the Seebeck effect). Figure 3.17 shows the setup of a basic thermocouple where the connected ends, T_{jct}, and the separated ends, T_{ref} of the two metals, A and B, are at different temperatures. This difference will produce a low-level DC voltage, E, at the +/- terminals.

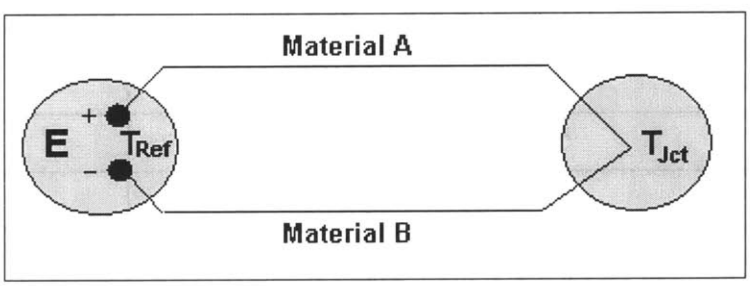

Figure 3.16- Simple Thermocouple (Moffat, 1997)

Theoretically, the voltage value E can be calculated from the following equations (Moffat,1997), where ε_A and ε_B are the Seebeck coefficients (thermoelectric sensitivities).

Generally,

$$E = \int_0^L \varepsilon_A \frac{dt}{dx} dx + \int_L^0 \varepsilon_B \frac{dt}{dx} dx \qquad \text{Equation (3.34)}$$

The system can be simplified if we assume that the temperature in both wires begin at T_{ref} and end at T_{jct}. Equation (3.34) then becomes:

$$E = \int_{T_{ref}}^{T_{jct}} (\varepsilon_A - \varepsilon_B) dt \qquad \text{Equation (3.35)}$$

For small temperature differences, we can further simplify equation (3.34) by assuming the values of ε_A and ε_B to be constant:

$$E = (\varepsilon_A - \varepsilon_B)(T_{jct} - T_{ref}) \qquad \text{Equation (3.35)}$$

The Seebeck coefficient for some common materials is listed in Table 3.4 (Thermocouple Theory, 2001)

Material	**Seebeck Coeff (μV/°C)**	**Material**	**Seebeck Coeff (μV/°C)**
Aluminum	3.5	Iron	19
Bismuth	-72	Lead	4.0
Carbon	3.0	Nickel	-15
Constantan	-35	Platinum	0
Copper	6.5	Silver	6.5
Gold	6.5	Tungsten	7.5

Table 3.4 – Seebeck Coefficients

3.5.2 Thermocouple Types

Thermocouples are categorized by the combination of materials used. The three most common thermocouple alloys for moderate temperatures, as described by Moffat are Iron-Constantan (Type J), Copper-Constantan (Type T), and Chromel-Alumel (Type K).

Iron-Constantan (Type J) – Generates about 50μV/°C (28μV/°F). The iron wire is magnetic and junctions can be made by welding or soldering. Type J thermocouples should not be used for wet conditions, since the combination of iron and constantan can generate a galvanic EMF between the two wires in the presence of water. The operating temperature range for type J is –210 to 1200 °C (-350 to 2200 °F).

Copper-Constantan (Type T) – Generates about 40μV/°C (22μV/°F). Neither copper nor constantan is magnetic and junctions can also be made by welding and soldering. Due to the high thermal conductivity of copper, type T thermocouples are very susceptible to conduction error. Type T's temperature range is –270 to 400 °C (-450 to 750 °F).

Chromel-Alumel (Type K) – Also generates about 40μV/°C (22μV/°F). The alumel wire is magnetic and high temperature silver-solders and special fluxes must be used in the welding or soldering process. Type K thermocouples can generate electric signals when the wires are bent and therefore should not be used on vibrating systems. The functioning temperature variations for type K are –270 to 1350 °C (-450 to 2500 °F). Using a type K in high temperatures should be monitored closely as 5°C drifts have been reported around 1000 °C (Polak, 1999). In these circumstances a type N (chromium/nickel and silicon/nickel) may be appropriate. A conceptual model of a type K thermocouple is shown in Figure 3.18.

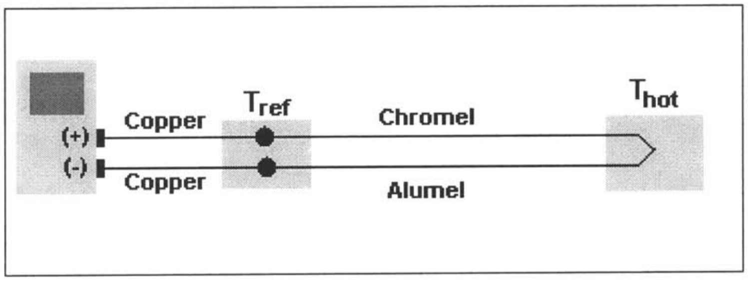

Figure 3.17 – Type K thermocouple (Moffat, 1997)

3.5.3 Thermocouple Wiring

Three grades of wire are available in each thermocouple type: Precision, Standard and Lead-Wire, with varying calibration percentages:

Wire Grade	Calibration Percentage
Precision	Larger of: +/- 3.8 % or 1°C (2°F)
Standard	Larger of: +/- 3.4 % or 2°C (4°F)
Lead-Wire	+/- 1.0 %

Table 3.5 – Calibration percentage of wire grades

3.5.4 Thermocouple Junction

Thermocouple probes are available in three junction types: grounded, ungrounded and exposed (<u>How Thermocouples Work</u>, 2001). In a grounded junction, the thermocouple wires are physically attached to the inside of the probe wall, resulting in good heat transfer through the probe wall. Ungrounded junctions have a separation between the wires and the wall. This leads to slower response times, but better electrical isolations. Finally, exposed junctions have an opening in the probe wall to expose the thermocouple wires. Consequences are faster response times, but corrosion can occur through time.

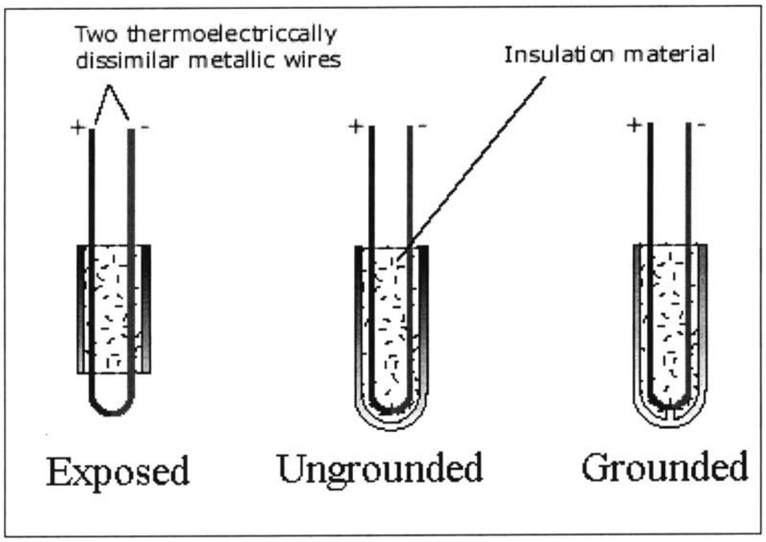

Figure 3.18 – Thermocouple Junctions (Thermocouple Introduction, 2001)

3.5.5 Alternative Technology

An alternative to using thermocouples is a Resistance Temperature Detector (RTD) (Polak, 1999). These devices function on the fact that the resistance of metals increases with temperature. This relationship is shown in Figure 3.20 for several RTD materials. The most common metal used in RTD manufacturing is platinum.

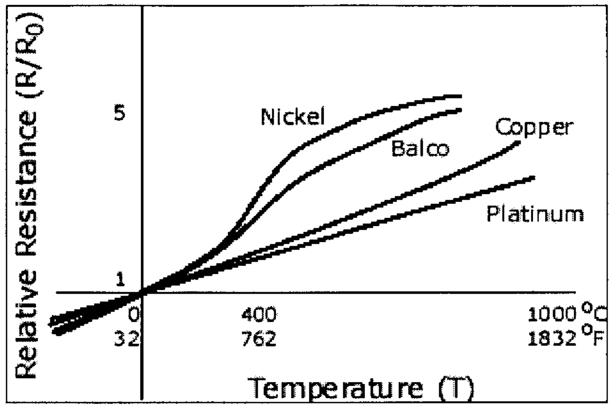

Figure 3.20 –Temperature – Resistance Relationship
(Resistance Temperature Detector : Theory, 2001)

Notice from figure 3.20 that most materials have a range where the relationship is linear. In these regions the temperature, as a function of the resistance, can be written as (Resistance Temperature Detector : Theory, 2001)

$$T = T_{ref} + \frac{\left(R / R_{ref} \right) + 1}{\alpha} \qquad \text{Equation (3.36)}$$

where α is the slope of the Resistance-Temperature line.

RTD's are more stable and accurate than thermocouples since the size of the bulb (measuring end) automatically incorporates some temperature averaging, unlike the tip-sensitive thermocouples. Normally bulbs are around 25 mm long and are fully covered by stainless steel sleeves, slowing their response time. Some versions have small holes in the sleeve to allow for circulation. In general RTD's have better long-term stability and are less susceptible to electrical noise (Polak, 1999).

4 MEMS Technology

4.1 Background

Before the availability of microelectronics, most sensors were usually combined directly with an output device, typically a meter that was recorded by an engineer. There are still many devices today that are read in such fashion like a home thermostat or factory flow meters. The advancement in microprocessor technology assisted in the vision that sensors could have built-in electrical outputs that could provide unattended measurement and control.

The transition from mechanical to electronic sensing is evident in the evolution of position measuring devices. Variable reluctance measurements with magnetic pickups have been replaced by Hall effect, opto sensing and magneto resistive (MR) elements. These techniques use semiconductor technology to solve the sensitivity problems that transistors had to temperature, light, magnetic fields and stress (Frank, 1996). The growing number of parameters that can be sensed with semiconductor technology has furthered the interest in smart sensing. Outlined below are the development stages that sensors have gone through in reaching a complete electronic sensing solution:

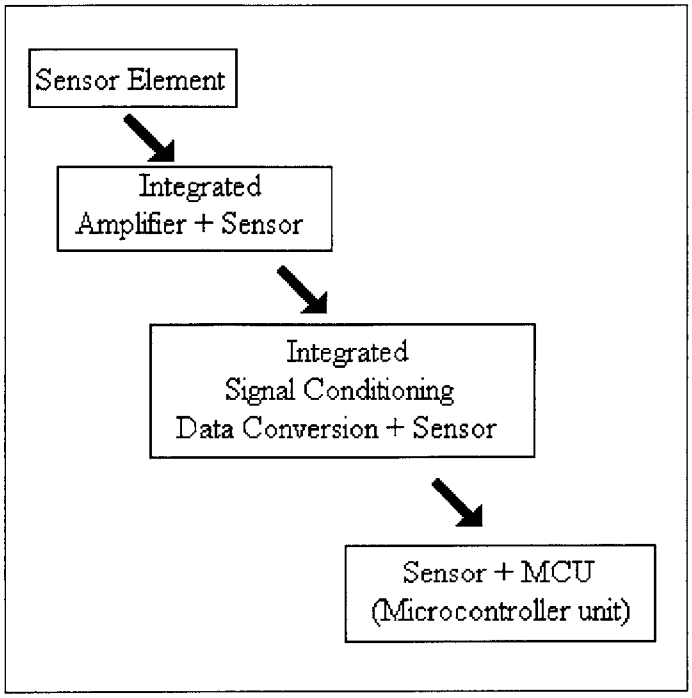

Figure 4.1 – Stages of Increased Integration (Frank, 1996)

4.2 MEMS Technology

A major advancement toward the future of smart sensing is MEMS technology. MEMS (Micro-Electro-Mechanical-Systems) is the integration of mechanical elements, actuators, and electronics on a common silicon substrate through the use of micro fabrication technology. The combination of microelectronics with micromechanical structures opens the door for revolutionizing control systems. In their most basic form, sensors gather information from the environment through measuring mechanical, thermal, biological, chemical or optical properties. Combining on-board electronics, the information gathered can be processed and through some intelligent algorithms direct the physical event that is being monitored. In terms of MEMS, this means directing the microactuators to respond by moving, positioning, regulating, and filtering, thereby controlling the environment for some desired outcome.

The induction of microelectronic integrated circuits (ICs) into sensors further develops the ability to intelligently control the environment. MEMS devices are manufactured using the same techniques as integrated circuits, increasing their functionality and lowering production costs. Section 4.4 will cover in greater detail the manufacturing methods that allow miniature components to be created. It is often confusing to what MEMS actually refers to. MEMS technology does not refer to producing small parts or making components out of silicon. What categorizes MEMS is the manufacturing technology behind the creation of these sensors (What is MEMS Technology?, 2001). It not only has the capacity of creating miniature components, as in the motor pictured in Figure 4.2 (Hui, 2001), but of mass-producing components.

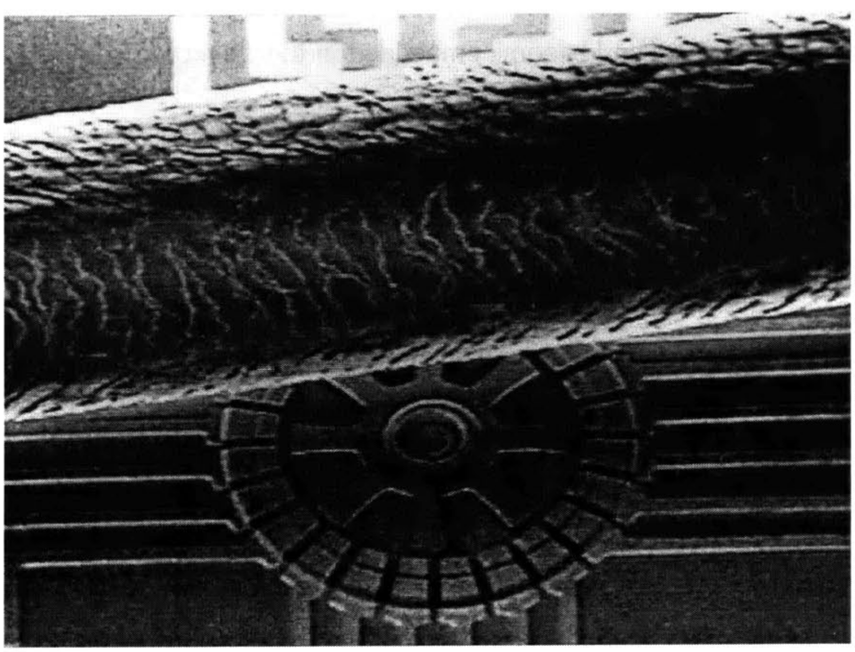

Figure 4.2 – Silicon MEMS motor next a strand of human hair (dia. ≅ 100 microns)

There are many advantages to using MEMS technology driven sensors (What is MEMS Technology?, 2001). For one, MEMS is extremely diverse. The range of applications is still unknown, as the medical, military and manufacturing fields are only discovering the limitations of this technology. A successful MEMS company will not survive with only programmers, like the semiconductor industry, they will need to unify several engineering disciplines with physicists and even biologists (Finke, 2000). MEMS has also erased the lag that complex mechanical systems placed on electronic circuit integration. Through batch manufacturing, the mechanical components no longer are the weak link in terms of cost and reliability.

The future of MEMS appears very bright. Many people believe that the MEMS industry is in the same stage as the semiconductor industry was in 35 years ago (Finks, 2000). Their similar mass-producing capabilities is a sign that MEMS could grow very rapidly in the next 35 years and become embedded in most everyday devices.

4.3 Silicon based

Almost every MEMS component is manufactured from silicon. Its strength-to-weight ratio is higher than most other engineering materials, making it ideal for producing mechanical structures. Silicon's modulus of elasticity is close to that of steel, while its yield strength is higher than both steel and aluminum (Frank, 1996). The electrical properties of silicon are also favorable for integrated circuits, though not many MEMS devices have exploited both the mechanical and the electrical properties.

Property	Silicon	Stainless Steel	Aluminum
Young's Modulus (10^{12} dyn/cm^2)	1.9	2.0	0.7
Yield Strength (10^{10} dyn/cm^2)	6.9	2.1	0.17

Table 4.1 – Silicon/Steel/Aluminum Comparison (Frank, 1996)

Silicon does encounter some problems in high temperatures. Plastic deformation can begin occurring at 600 °C. While its fracture strength is reported to be 7000 MPa, some anisotropically etched diaphragms have failed as low as 300 Mpa. Research revealed that the sharp corners in anisotropically etched specimens contained stress concentration factors of nearly 33. Rounding of corners by isotropic etching showed a reduction in the stress concentration factor resulting in higher load resistance (McEntee, 2001). Some alternative materials that are being experimented include using either diamond or polymer films (Frank, 1996).

4.4 Micromachining techniques

Micromachining is a chemical etching process for manufacturing three-dimensional microstructures, similar to semiconductor processing techniques. The advancements of micromachining are causing re-evaluations of several scientific and engineering fields. Bulk micromachining has been used to manufacture semiconductor pressure sensors since the late 1970's. Recently, newer techniques such as surface micromachining have been developed that can produce even smaller components.

4.4.1 Bulk Micromachining

Bulk micromachining is a process that allows the mass production of three-dimensional microstructures out of silicon wafers. The basic process consists of etching a masked silicon wafer in an orientation-dependent etching solution (Frank, 1996). Using micromachining technology, several wafers can be fabricated simultaneously and batch consistency is maintained through a small number of parameters, such as the crystallographic orientation, etchant concentration, semiconductor starting material, temperature and time. In the etching procedure different types of silicon may be used for controlling the incision. N-type silicon is etched 50 times faster than P-type, therefore N-type is often used as a starting material. P-type can then be grown or diffused into the wafer as a stopping mechanism in the cutting process (Frank, 1996). An advantage in using bulk micromachining is that the etching procedure is stress free. Table 4.2 shows different etching rates and how they depend on the material being etched and the etchant material.

Etched Material	Etch Rate (nm/min)	Etchant
Al	80	$SiCl_4$
Polysilicon	60	$SiCl_4$
SiO_2	25	$SiCl_4$
ZnO	5	$SiCl_4$
Si	900 – 1,300	SF_6
Si	10,000 – 300,000	HF

Table 4.2 – MEMS etching material (Frank,1996)

4.4.2 Surface Micromachining

Surface micromachining is a procedure where layers of structural material and sacrificial material are deposited over a substrate for selective etching. Common structural and sacrificial material combinations include polysilicon and silicon dioxide. As seen in the figure below, the sacrificial material acts as an intermediate space layer and is etched away to produce a freestanding structure.

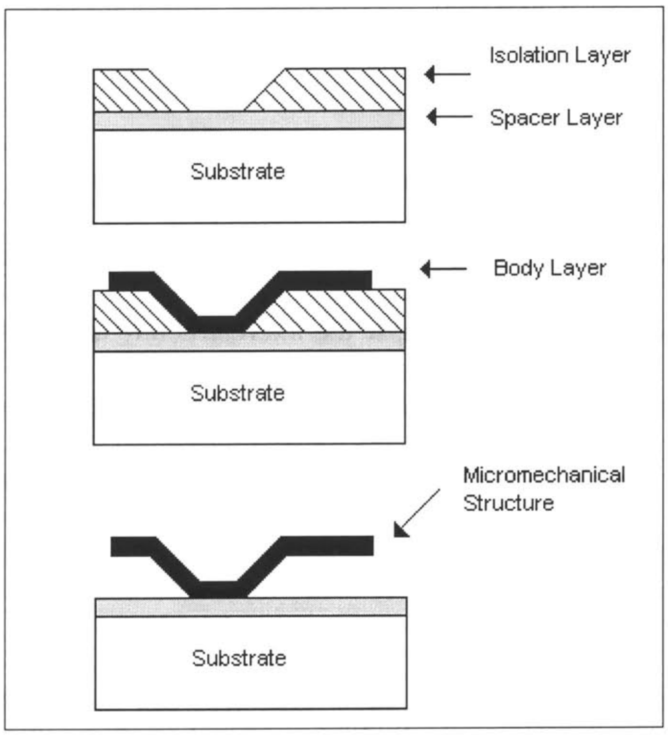

Figure 4.3 – Surface Micromachining Sequence (Frank, 1996)

Smaller and more complex structures are achievable with surface micromachining. Typical spacing between components is 2 μm. Unlike bulk micromachining, stresses can build up in the layers during and after the removal of the sacrificial materials and lead to warping. Surface micromachining also faces problems with squeeze-film damping, static friction and particle contamination, which must be dealt with in each design (Frank,1996).

Squeeze-film damping is a dynamic damping effect that two microstructures encounter when they are spaced only a few microns from each other. The gas separating the faces has a viscous damping constant that increases with the inverse cube of the spacing (Frank, 1996). To solve this problem, holes are made in the surface of the microstructure to control the damping effect. The incision of holes also provides a means of access for the etchant, resulting in reduced etching times.

Static friction, also known as stiction, can occur when capillary forces are generated during the wet-etching of the sacrificial layers. These forces combined with certain fabrication conditions can collapse the microstructure and cause it to permanently adhere to the substrate. Preventing the presence of capillary forces when the etching liquid is removed varies between the product designed and the process flow (Frank, 1996).

The close separation between microstructures can also lead to contamination. While sensors as a whole are protected by an outer package, the solution to contamination is to incorporate packaging at the wafer level. Packaging individual microstructures prevents contamination from microscopic particulates and handling, and also manages the ambient temperature for damping control. Common packaging materials include epoxy, metals and ceramics (Frank, 1996).

4.5 MEMS Accelerometers

MEMS accelerometers use micromachining technology to produce an inexpensive alternative to conventional accelerometers. The automotive industry has quickly incorporated MEMS accelerometers into cars for driving management, safety and comfort. In the field of safety, these devices are currently used in air-bag deployment systems. While some cars use a system with separate accelerometers and electronics, the MEMS alternative combines the two into a single silicon chip for one-fifth of the price. The low cost and compact size of these devices are advancing safety levels by allowing cars to have side door airbag deployment systems as well. Future improvements to MEMS accelerometers expect to give the sensors the ability to determine the size and weight of a passenger. This information can be used to optimize the system response and reduce the possibility of air-bag deployment related injuries (What is MEMS Technology?, 2001).

In relation to the Flagpole project, the ability of having an inexpensive sensor that is practically undetectable to a common passerby would solve several issues currently facing the team. First, the installation of sensors on exterior faces of structures affects their aesthetic quality. Depending on the location and importance of the structure, defacing it with sensors and wires may not be an option. MEMS accelerometers, however, can be fabricated in such small scales that they would virtually go undetectable. Second, the low cost would allow for sensor networks to be installed. Increasing the number of sensors would result in a system redundancy for crosschecking results. For the flagpole specifically, a network of sensors can increase the value of structural analysis being made on the flagpole. Different bending modes will be captured more easily and a more precise displacement distribution will be plotted.

While there are many benefits in setting up sensor networks, a hindering feature would have to be the wiring required in sending the sensor's signal to a data acquisition system. A network of wires would surely disturb the structures facing. For this reason, Chapter 5 will investigate the recent developments in the area of wireless sensor networks.

5 Wireless Sensor Networks

5.1 Overview

As seen through the advances of MEMS, sensor technology is definitely reaching new milestones and making its way into new, never imagined applications. While technology has attacked many of the drawbacks of old sensor technology: size, cost, durability and need of external data processing, one feature is hindering the unlimited applications of sensors in today's world. This feature is wireless transmission. If sensors could broadcast to great lengths with low power requirements, amazing breakthroughs in the area of monitoring could be achieved.

5.2 WINS

5.2.1 Introduction

Progress toward achieving the integration of MEMS sensors and wireless communication has been made lately in an area of research known as WINS (Wireless Integrated Network Sensors). The goal of WINS is to provide a distributed network and Internet access to sensors, controls, and processors that are deeply embedded in equipment, facilities, and the environment. This is achieved by combining microsensor technology, low power signal processing, low power computation, and low power wireless networking capability in a compact system. WINS networks will provide sensing, local control, and embedded intelligent systems in structures, materials, and environments.

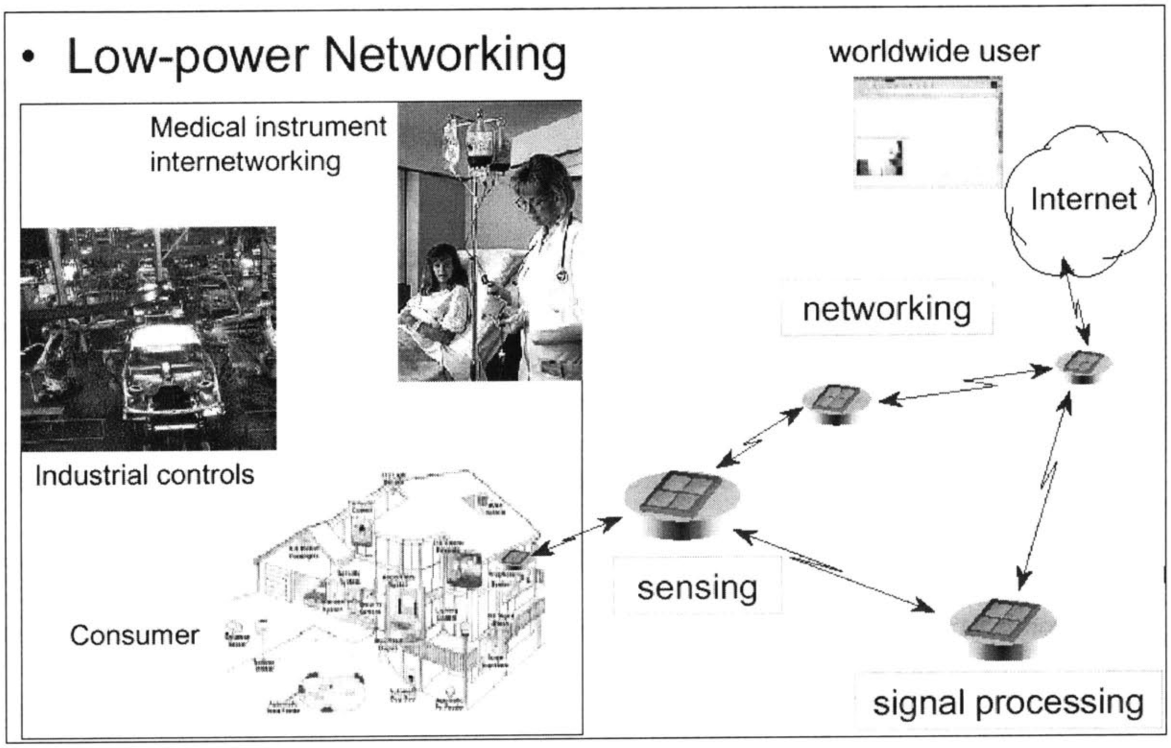

Figure 5.1 - WINS system diagram (WINS, 1998)

According to a research group at UCLA, the fields that will feel the greatest impact of distributed wireless MEMS are mechanical, industrial, and civil engineering. In industrial engineering, WINS will provide engineers with new methods to monitor cost and product quality. In the manufacturing process, WINS hopes to revolutionize control systems, where distributed sensors monitor and provide feedback throughout the manufacturing cycle. Finally, civil engineering will use MEMS to monitor structures through its life cycle, from construction to demolition (WINS, 1998).

5.2.2 Wireless Requirements

WIMS technology is based on low power solutions to communication systems. The term used to describe this focus of WIMS is LWIM (Low Power Wireless Integrated Microsensors). There are three major requirements in a LWIM system. First, there are strict power requirements. Second, the data transmission rate must be reduced. Third, node-to-node link budget is relaxed. Table 5.1 shows a complete list of specifications of LWIM systems:

	Specifications
Operation Frequency	ISM band (902-928 MHz)
Channel Spacing	500 kHz
Tone Frequency	100 kHz
Data Rate	1~ 100 kbps
Frequency Accuracy	20 ppm
Current Consumption	~ 1 mA

Table 5.1 – LWIN specifications (WINS, 1998)

5.2.3 Applications scales of WINS

The use of distributed MEMS is going to shift our information systems from a user-to-user network to a user-to-physical world network. Users will then have the ability to remotely monitor and control the physical environment from a global scale to a local machine scale. Examples of WINS's role in different monitoring scales are shown below (WINS, 1998):

- Global scale - WINS will allow monitoring of land, air and water resources.

- National scale - transportation systems and borders will be monitored for efficiency, safety, and security.
- Metropolitan scale - new traffic, security, emergency, and disaster recovery services.
- Local enterprise scale - WINS will create a manufacturing information service for cost and quality control. In biomedicine hospital patients and medical professionals will be connected through sensing, monitoring, and control.
- Local machine scale - WINS condition-based maintenance devices will equip power plants, appliances, vehicles, and energy systems for enhancements in reliability, reductions in energy usage, and improvements in quality of service.

5.2.4 Examples

Medical Informatics

The medical field deals with large amounts of information daily, some of which is life-critical. The ability to monitor patients and medical equipment in real-time has brought sensor technology into hospitals and clinics. Furthermore, WINS is allowing monitoring to take place not only in clinical environments, but also for ambulatory outpatients in their homes.

Information Systems for National Security

The Presidential Commission on Critical Infrastructure Protection has recently raised the awareness that our nation's most critical infrastructures are vulnerable to physical and cyber threat (WINS, 1998). These sectors include telecommunications, energy, banking and transportation. In order to safeguard power, water and transportation services, diverse sensor measurement capabilities will be required. The low cost of distributed MEMS makes it an ideal technology to build this detection information service.

<u>Military</u>

The US Marine Corps and the US Navy have both actively participated in researching applications for wireless sensor networks. WINS have been used in battlefield simulations to provide tactical information through acoustic, magnetic, and image processing. The placement of WINS sensors can be done through airdrop, inserted by artillery, and carried individually. In order to keep costs down and retain a scalable system, local processing of the data is required. The savings occur because the threats are identified and the decision-making is done at the remote sensor location. Thus, instead of sending all information to a master terminal for analysis, only the decision and relevant data is necessary, reducing the hardware and human assistance needed to monitor the sensor network

5.3 Bluetooth Technology

5.3.1 Introduction

Bluetooth is a wireless technology that gives various communication devices, such as mobile phones and desktop and notebook computers, the capacity to make instant and wireless connections. Bluetooth is not a particular product; it is an invisible technology made of specifications for short-range radio links between mobile PC's, mobile phones and other portable devices. These standards for communication are set by a group of leaders in the telecommunications, computing, and networking industries, known as the Bluetooth Special Interest Group.

The goal of the Bluetooth Special Interest Group is to promote an open, royalty-free specification for seamless wireless connectivity and cable replacement for a wide variety of mobility-enhancing devices. At no cost, any company may join the group and obtain a royalty-free license to develop and manufacture products based on Bluetooth wireless technology. The founders of the group include Ericsson Mobile, IBM Corp, Intel Corp, Nokia Mobile and Toshiba Corp. To date there are nearly 2500 members (Bluetooth, 2001).

5.3.2 Bluetooth Standards

The appeal of Bluetooth in the field of sensor networks is that it can replace multiple cable connections via a single radio link. The use of radio transmission allows the transfer of both voice and data in real-time. The Bluetooth standard is based on a frequency hopping scheme operating in the 2.45 GHz band. Applications utilize power levels from 0 to +20 dBm (for ranges covering 10 to 100 m) (Browne, 2000). As a side note, Bluetooth has been banned in France because the French military used the 2.4 GHz range in their communication devices (Fuhr, 2001).

Most communication systems have avoided the 2.4 GHz range because of high noise levels and signal corruption. The hopping scheme helps Bluetooth operate effectively in noisy environments. After each transmittal the frequency hops at a maximum rate of 1600 hops/second with hops occurring in 1 MHz increments.

Bluetooth's standard supplies a spectrum of 79 slots; therefore the operating frequency range is effectively 2.402–2.480 GHz. The use of short data packages and the implementation of forward error correction (FEC) are also reasons why Bluetooth is able to overcome random noise in the range of 0-10 meters (Fuhr, 2001).

The Bluetooth wireless technology supports both point-to-point and point-to-multipoint connections. With the current specification, up to seven 'slave' devices can be set to communicate with a 'master' radio in one device. Several of these 'piconets' can be established and linked together, allowing communication among flexible configurations. All devices in the same piconet have synchronized priority, but other devices can be set to enter at any time (Bluetooth, 2001).

5.3.3 Bluetooth Applications

A Bluetooth radio is built into a small microchip and operates in a globally available frequency band ensuring communication compatibility worldwide. The Bluetooth specification has two power levels defined. A low power level covers a shorter personal area, such as a room, and a higher power level covers a medium range, such as within a home (Bluetooth, 2001).

5.3.4 Bluetooth vs. LWIM

Table 5.2 is a comparison of cellular, Bluetooth and LWIM technology. Notice that Bluetooth can handle 10 times the data rate than LWIM technology, but ends up using 20 times the power.

	Cellular	Bluetooth	LWIM
Noise Figure	8dB	26dB (estimate)	~25dB
Sensitivity	-102dBm	-70dBm	~80dBm
Data rate	~10kbps	1Mbps	≤ 100kbps
Current consumption	35 – 40 mA	≤ 20 mA	~ 1 mA

Table 5.2 – Wireless comparison (WINS, 1998)

6 Conclusion

The Flagpole project has provided MIT with a solid foundation to continue developing their studies in real-time monitoring systems. The ability to interact with the latest technology helped the group understand the current industry limitations and reactively provide custom solutions to some problems. Some areas of the project that are in the forefront of technology, such as wireless transmission, are waiting for new industry releases. In particular, a Bluetooth solution with transmission ranges of up to 100 meters is soon to be released.

Once the initial phase of the project is complete and the accelerometers, strain gauges and thermocouples are in place and properly functioning, the Civil Engineering Department has its sights on the possibility of installing MEMS sensors on the flagpole. While the current accelerometer in use is based on MEMS technology, its package is still too bulky to go unnoticed by observers. These issues will hopefully lead into the use of wireless solutions such as WINS.

With the strong ties that academic institutions like MIT have to the professional world, an aspiration of this project is that these two fields can mutually influence each other in their monitoring practices. While MIT can provide companies with feedback on issues dealing with the latest technology being researched and also with custom software interfaces, companies can provide MIT with research funding and insights into practical issues faced with monitoring.

In order for the widespread sensors implementation in civil engineering to occur, companies and government agencies must be convinced that the cost of installing these sensor systems will not be comparable to the savings if catastrophic failure can be prevented. The real success, from a civil engineering perspective, of the advances in sensor technology will come if a building or a bridge can react instantaneously to an extreme physical force and prevent failure and fatalities. Once this occurs the development of distributed sensor technology will be looked upon as a breakthrough in engineering practices.

References

[1] Accelerometers. 2001. Analog Devices. 10 May 2001. <http://www.analog.com/imems>.

[2] Accelerometer Overview. 2001. Crossbow Technology. 10 May 2001. < http://www.xbow.com/>.

[3] Bluetooth. 2001. The Official Bluetooth Website. 10 May 2001. < http://www.bluetooth.com>

[4] Brignell, John and Neil White. Intelligent Sensor Systems. London: The Institute of Physics, 1994.

[5] Browne, Jack Wireless Sensors Leverage Bluetooth Communications Standard Wireless Systems Design July 2000 10 <http://www.planetee.com /planetee/servlet/DisplayDocument?ArticleID=479>

[6] Chopra, Anil K. Dynamics of Structures – Theory and Application to Earthquake Engineering. Upper Saddle River, NJ: Prentice Hall, 1995.

[7] Izmit, Turkey Earthquake Briefing 3 Sept 1999. EQE International. 10 May 2001. <http://www.eqe.com/revamp/izmitreport>.

[8] FieldPoint from National Instruments – Modular Distributed I/O System 2001. National Instruments. 10 May 2001. < http://www.ni.com/fieldpoint>.

[9] Finke, Douglas. MEMS Are Changing The Rules. ECN Special Report. May15 2000.

[10] Flagpole Project 15 Jan 2001. MIT Civil Engineering Dept. 10 May 2001. <http://flagpole.mit.edu>

[11] Fraden, Jacob. AIP Handbook of Modern Sensors: Physics, Design and Applications. New York: American Institute of Physics, 1993.

[12] Frank, Randy. Understanding Smart Sensors. Norwood, MA: Artech House, 1996.

[13] Fuhr, Peter L. Bluetooth. 11 May 2001. <http://www.sensorsmag.com /articles/0800/90/main.shtml>.

[14] How Thermocouples Work. NPH - National Plastic Heater Sensor and Control. 7 May 2001 < http://www.nphheaters.com /technical/thermo_letter.htm>.

[15] Hui, Elliot. Micromechanical Systems. 7 May 2001.<http://www-bsac.EECS. Berkeley.EDU/~elliot/mems.html>

[16] McEntee, Jarlath Properties of Silicon 7 May 2001 <http://design.caltech.edu /Research/MEMS/siliconprop.html>

[17] Moffat, Robert J. Notes on using thermocouples. Jan 1997 Electronics Cooling 29 March 2001 < http://www.electronics-cooling.com/Resources/EC_Articles /JAN97/jan97_01.htm>.

[18] Morris, Alan S. Principles of Measurements and Instrumentation. Hertfordshire, England: Prentice Hall, 1993.

[19] National Research Council. Expanding the Vision of Sensor Materials, Washington D.C : National Academy Press, 1995.

[20] Ohba, Ryoji. Intelligent Sensor Technology. West Sussex, England: John Wiley & Sons, 1992.

[21] Polak, T.A. and C. Pande. Engineering Measurements - Methods and Intrinsic Errors. Suffolk, England: St Edmundsbury Press, 1999.

[22] Popov, Egor P. Engineering Mechanics of Solids New Jersey: Prentice Hall, 1990.

[23] Putnam, William and R. Benjamin Knapp. Input/Data Acquisition System Design for Human Computer Interfacing 1996. 10 May 2001 < http://www-ccrma.stanford.edu /CCR.MA / Courses /252/sensors/sensors.html>

[24] Resistance Temperature Detector : Theory. 2001. Efunda. 10 May 2001. < http://www.efunda.com/designstandards/sensors/rtd/rtd_theory.cfm>

[25] Romberg, T.M., J.L. Black and T.J. Ledwidge. Signal Processing for Industrial Diagnostics. West Sussex, England: John Wiley & Sons, 1996.

[26] Strain Gage – Pattern. 2001.Efunda 7 May 2001 <http://www.efunda.com /designstandards/sensors/strain_gages/strain_gage_selection_pattern.cfm>

[27] Strain Gage- Sensitivity. 2001. Efunda. 7 May 2001 <http://www.efunda.com/ designstandards/ sensors/strain_gages/strain_gage_sensitivity.cfm>.

[28] Thermocouple Introduction. Efunda. 7 May 2001. <http://www.efunda.com/ designstandards/sensors/thermocouples/thmcple_intro.cfm>.

[29] Thermocouple Theory. 2001. Efunda. 7 May 2001. <http://www.efunda.com /designstandards/sensors/thermocouples/thmcple_theory.cfm>.

[30] What is MEMS Technology? 19 April 2001. MEMS Exchange. 7 May 2001. < http://mems-ex.cnri.reston.va.us/about/what-is.html>.

[31] Wheatstones Bridges – Introduction. 2001.Efunda. 7 May 2001 <http://www.efunda.com/ designstandards/sensors/methods/ wheatstone_bidge.cfm>

[32] WINS. 4 Dec 1998. UCLA Electrical Engineering Department. 10 May 2001. <http://www.janet.ucla.edu/ WINS/wins_intro.htm #Introduction>